SPACE-BASED SOLAR POWER CONVERSION AND DELIVERY SYSTEMS STUDY

VOLUME IV

ENERGY CONVERSION SYSTEMS STUDIES

(NASA-CR-150297) SPACE-BASED SOLAR POWER CONVERSION AND DELIVERY SYSTEMS STUDY. VOLUME 4: ENERGY CONVERSION SYSTEMS STUDIES Final Report (Little (Arthur D.), Inc.) 74 p HC A04/MF A01 CSCL 10B G3/44

N79-22620

Unclas 19218

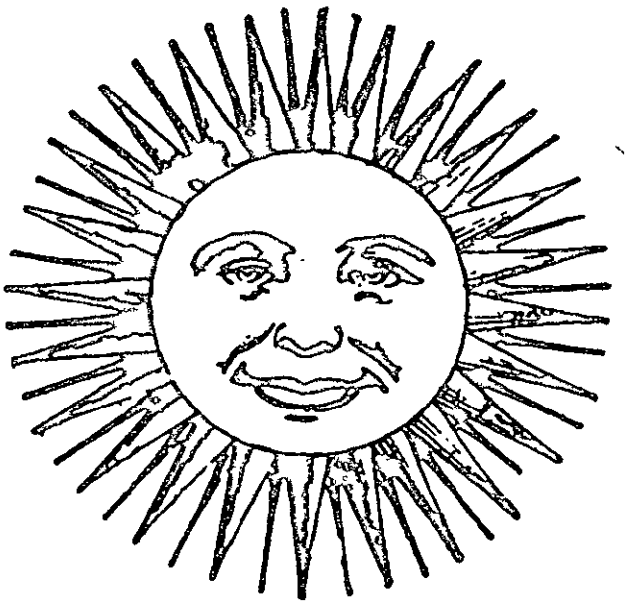

SPACE BASED SOLAR POWER CONVERSION AND DELIVERY SYSTEMS STUDY

FINAL REPORT

VOLUME IV

ENERGY CONVERSION SYSTEMS STUDIES

Prepared for

ECON, Incorporated
Princeton, New Jersey

C-78127

March 29, 1977

Arthur D Little, Inc.

PREFACE

The purpose of the work undertaken in this task was to examine solar cells and optical configurations for the SSPS other than silicon cells at a theoretical concentration ratio of two that had been previously considered in the analyzed configuration. Single crystal silicon is a proven solar cell material with a history of measured orbital performance data and was an obvious choice for the initial photovoltaic SSPS system studies. In response to the National Photovoltaic Conversion Program initiated in 1975 by ERDA, active research in photovoltaic materials and improved solar cell technology has produced an increasing number of promising alternative materials applicable to the solar energy conversion subsystem for the SSPS.

In this task, three specific solar cell materials were examined: single crystal silicon, single crystal gallium arsenide, and polycrystalline cadmium sulfide. The comparison of the three different cells on the basis of a subsystem parametric* cost per kW of SSPS-generated power at the terrestrial utility interface showed that gallium arsenide was the most promising solar cell material at high concentration ratios. The most promising solar cell material with no concentration, was dependent upon the particular combination of parameters representing cost, mass and performance that were chosen to represent each cell in this deterministic comparative analysis. The potential for mass production, based on the projections of the present state-of-the-art (which were not quantified in this effort) would tend to favor cadmium sulfide in lieu of single crystal silicon or gallium arsenide solar cells.

This work was performed at Arthur D. Little, Inc., under the direction of Dr. Peter E. Glaser. Dr. David W. Almgren, Dr. Edward J. Cook, Jr., Mr. Arthur D. Gaudet, and Mr. William J. Raymond contributed to selected aspects of this task.

---

*Parametric cost as used here includes the capital cost of the solar cells, optical reflectors and basic support structure, as well as the transportation cost to GEO for the cell reflectors and basic support structure of the SSPS.

 PRECEDING PAGE BLANK NOT FILMED

TABLE OF CONTENTS

TABLE OF CONTENTS
(Continued)

LIST OF FIGURES

LIST OF FIGURES

LIST OF FIGURES

LIST OF TABLES

1. PURPOSE

1.1 Task Objectives and Scope

The objective of this task was to examine the relative merits of alternative photovoltaic solar energy conversion subsystems for the SSPS in addition to the silicon cells with a theoretical concentration ratio of two previously used in the analyzed SSPS configuration. This study considered specific silicon, gallium arsenide and cadmium sulfide solar cells over a theoretical concentration ratio range of 1.0 to 8.0. The effort focused on systems with passive cooling although consideration was given to a simple design using augmented cooling.*

Based upon the original, analyzed SSPS configuration, which used a theoretical concentration ratio of two, data were developed that represented pessimistic, most likely and optimistic values for the projected conversion efficiency of specific solar cells as well as their array mass and cost per unit area for the 1990's time period. In addition, an algorithm was developed that computed the rate of degradation of solar cell efficiency caused by radiation damage as a function of time in GEO. This set of data was utilized by ECON to perform a cost/risk comparative analysis of the baseline SSPS for the three specific solar cell materials.

---

*As used here "augmented cooling" refers to a thermal design that uses radiating areas for cooling of the solar cells in addition to the front and back surfaces of the solar cell array.

2. BACKGROUND

2.1 Relationship of Current Study to Overall ECON Program

The major effort undertaken in this task was independent of the further in-depth analyses of the analyzed SSPS configuration being undertaken by ECON and was directed to alternatives to the analyzed configuration in the area of solar cells (based on different materials) and solar concentration ratios (based on different optical configurations). To assess the impact on the analysis caused by a different choice of solar cell material required that the characteristics of the three different solar cells be determined for the optical configuration of the analysis.

The analyzed configuration has a fixed theoretical concentration ratio of 2.0 which is not the "optimum" (minimum parametric cost) concentration ratio for any of the three different cell materials investigated in this task. Variations in concentration ratio have significant effects on the design of the optical system and its support structure. Considerations of such variations in the ECON mathematical model would have resulted in a major impact on the details of the design and construction procedure for the already established analyzed configuration. Therefore, the results from this task were utilized in the ECON model at a fixed concentration ratio of two.

Both silicon and cadmium sulfide had a computed minimum parametric cost per kW of generated power at a theoretical concentration ratio of about 2.4, which is near the baseline value of 2.0. Gallium arsenide has a computed minimum parametric cost at a concentration ratio greater than 7.0 and, therefore, is operating furthest from its optimum design point when compared to the other solar cells in the baseline configuration.

2.2 Discussion of the Analyzed SSPS Configuration

Figure 2.1 shows the analyzed SSPS configuration as it existed at the beginning of this task. This configuration was well defined and served as a departure point for the examination of alternative solar cells and concentration ratios. This task utilized the solar array output to utility interface efficiency chain (54.7%) as derived for the analyzed model and reported in Volume III of the Second Interim Report, to compute that 9.141×10^6 kW of dc electric power must be generated by the solar arrays at a specified point in time to be able to deliver 5.0×10^6 kW to the utility interface at the same point in time, e.g., 5 years into the life of the power station. In addition, the mass and cost per unit area of the concentrating optics (reflector surface area, not projected area) and the mass and cost per unit projected area of the basic SSPS support structure (supporting both the solar array and any associated optical system) were taken from the baseline configuration and used in this task as a constant multiplier times the total area

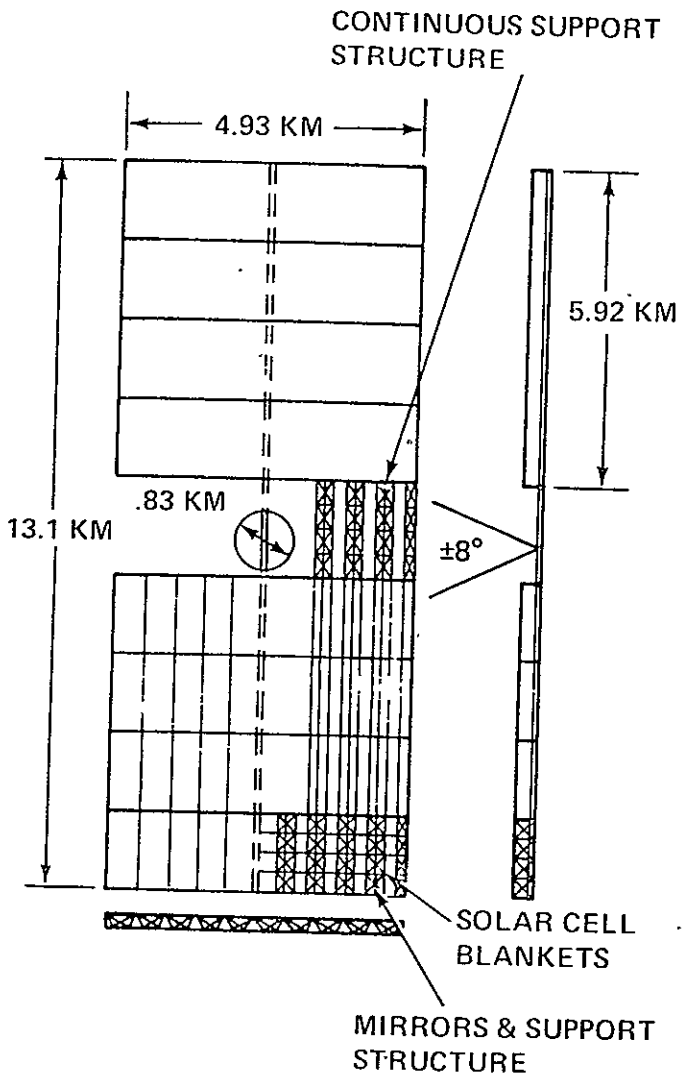

- CHARACTERISTICS
  - POWER — 5000 MW
  - WEIGHT — 18.1×10^6 KG
  - SIZE — 13.1 X 4.9 KM
  - ORBIT — GEOSYNCHRONOUS
  - LIFE — 30 YR
  - OPERATING FREQ — 2.45 GHZ
  - DC-TO-DC EFFIC — 58%

FIGURE 2.1 THE SATELLITE SOLAR POWER SYSTEM - ANALYZED CONFIGURATION AS IT EXISTED AT THE BEGINNING OF THIS TASK

of reflecting surfaces or support structure. The mass of the basic support structure included both conducting and non-conducting elements as defined for the analyzed configuration. The solar array, optical reflectors and basic support structure, which were the elements of the SSPS modeled in this task, comprise approximately 71% of the total mass of the analyzed configuration. The antenna structure is the most massive item not considered in this subsystem analysis, accounting for approximately 26% of the total analyzed configuration mass. The parametric cost values developed in this task for comparing the three different solar cells at the subsystem level did not include the fixed mass (5.720×10^6 kg) and fixed transportation cost to GEO for the antenna structure.

3. ASSUMPTIONS AND SUPPORTING DATA

3.1 Assumptions Inherent in Analyses

The assumptions inherent in the analytical model description of the solar energy conversion subsystem affect all aspects of the modeling of the hardware design of the SSPS as well as of the environmental parameters of the solar constant and the radiation fluence in GEO. A detailed statement of the assumptions inherent in these analyses is presented at this point, prior to a presentation of the results and conclusions of the analyses, because the results from the comparative analyses of the different solar cell materials are dictated by the parameters chosen to characterize the individual solar cells and to model selected aspects of the analyzed SSPS configuration. This section discusses the assumptions pertaining to fixed value parameters followed by variable parameters.

3.1.1 Fixed Value Parameters

The fixed value parameters are those which are independent of the choice of a particular solar cell material.

3.1.1.1 Analyzed Configuration Parameters

Table 3.1 summarizes the assumed fixed value parameters that were taken from the analyzed configuration. Of particular significance is the assumption that, as the concentration ratio varies, there are constant multipliers to determine the mass and cost of the basic support structure and optical reflectors, based only on total areas. A variation in concentration ratio could imply a redesign of the optical support structure to satisfy the change in system pointing and optical surface requirements. These considerations are not a part of the current analyses.

The mass per unit area for the support structure includes both conducting and non-conducting structures as defined for the analyzed configuration and is used in this analysis as a multiplier times the total projected area of the SSPS rather than just the solar array area.

3.1.1.2 Environmental Parameters

There are two significant assumptions regarding environmental parameters. The first is that a fixed design value for the solar constant of 1353 W/m^2 can be used in these analyses. The $\pm$ 3.4% annual variation in the solar constant, as shown in Figure 3.1, was recognized as producing a significant variation in the power that could be generated by the solar cells ($\pm$ 300 mW); however, for the stated purpose of comparing different solar cells, a fixed value was sufficient and the SSPS size and mass were computed based upon this fixed value.

Table 3.1 Assumed Fixed Parameters from Analyzed Configuration

Parameter	Fixed Value
Solar Constant	1353 W/m^2
Power Developed by Photovoltaics	9.141×10^6 kW
Mass/Unit Area Support Structure	21,300 kg/km^2
$/Unit Mass Support Structure	81 $/kg
Mass/Unit Area Reflectors	29,670 kg/km^2
$/Unit Area Reflectors	1.035×10^6 $/$km^2$
Transportation Costs to GEO	80 $/kg

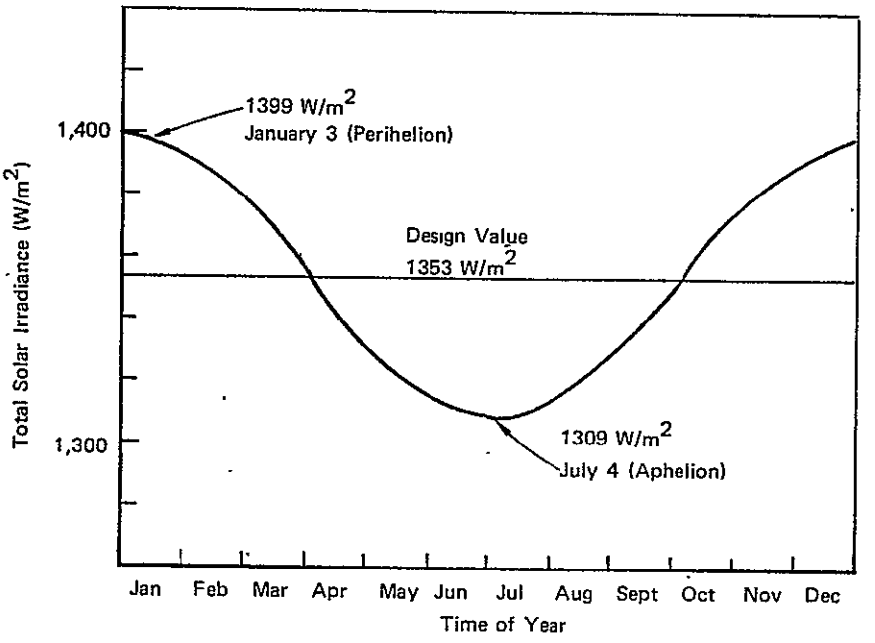

FIGURE 3.1 ANNUAL VARIATION IN TOTAL SOLAR IRRADIANCE (W/m^2) INCIDENT ON SSPS

The second assumption is that the rate of radiation damage to a solar cell at GEO can be computed based upon an equivalent fluence of 1 MeV electrons. For the seven year time period from 1970 to 1977, a total equivalent fluence of $3 \times 10^{14} e \cdot cm^{-2}$ was calculated for a silicon solar cell at synchronous altitude with a 300 μm coverslide [1]. This translates into an annual equivalent fluence of 1 MeV electrons of $.43 \times 10^{13}$ e · cm^{-2} per year and this was the common annual fluence used in these analyses to determine cell efficiency degradation due to radiation damage.

3.1.2 Variable Parameters

The variable parameters represent those aspects of the SSPS in the solar energy conversion subsystem that varied with a change in solar cell material or concentration ratio.

3.1.2.1 Photovoltaic Material Properties

Tables 3.2, 3.3, and 3.4 show the range of values of solar cell efficiencies, mass per unit area of the solar array and cost per unit area of the solar array, that were used for these analyses. Values were used in these subsystem level analyses in a deterministic sense while the full range of minimum to maximum values were utilized by ECON in the stochastic cost/risk analyses of the full SSPS system. The "maximum value" of assumed mass per unit area of the solar array for the silicon cell (300 μm cell, 150 μm coverslide) was utilized in the preliminary comparative analyses of the three different cell materials because it represents currently available solar cells. The initial, comparative computer runs showed that this current silicon cell had a parametric cost higher than the other candidate solar cells for the SSPS due to its large mass per unit area.

No attempt was made in this task to vary the coverglass thickness as a result of a trade study between the cell's mass and its rate of degradation of conversion efficiency in the GEO environment. As an indication of the complexity involved in computing an optimum coverslide thickness, Waddel's [2] experiment on ATS-1 indicated that cells covered with 150 μm Corning 7940 coverslide degraded least during the 416 day experiment. Cells with either thinner or thicker coverslides made of Corning 7940 or other glasses degraded more because of increased cell damage or coverslide loss. Anspaugh's [3] experimental silicon solar cell data from ATS-5 showed that after 699 days on orbit, an increase in cell coverslide thickness gave an increase in radiation protection of the cells but that this increase was small for cells with coverslides greater than 500 μm.

The conventional single crystal silicon solar cell was assumed to have a 150 μm coverslide of Corning 7940 (.033 g/cm^2) in these analyses. The current gallium arsenide solar cell was assumed to have a standard 125 μm FEP coverslide (.027 g/cm^2) and the cadmium sulfide cell was modeled as having a 25 μm layer of SiO_2 (.0065 g/cm^2)

Table 3.2 Assumed Solar Cell Efficiencies*

Solar Cell Material	Pessimistic (Today's Values)	Most Likely (Emerging)	Optimistic	Theoretical Limit
Silicon	12%	16%	19%	22%
Gallium Arsenide	14	18	22	27
Cadmium Sulfide	8	10	12	18

* Air Mass Zero at 26°C

Table 3.3 Assumed Mass/Unit Area of Solar Array (mg/cm^2)

Solar Cell Material	Minimum	Most Likely	Maximum
Silicon	28.2	40.0	115.0
Gallium Arsenide	33.2	43.2	52.6
Cadmium Sulfide	11.5	14.9	19.4

Table 3.4 Assumed Solar Array Costs ($\$10^6/km^2$)

Solar Cell Material	Minimum	Most Likely	Maximum
Silicon	48.7	86.6	730.6
Gallium Arsenide	48.7	203.0	1488.3
Cadmium Sulfide	48.7	86.6	270.6

for a coverslide based on a glass resin formulation process [4]. Recently published results from a NASA funded, TRW epxerimental program [5] have shown that heat laminated Teflon was not a promising material for use as a coverslide on an orbiting solar cell because of its embrittlement when exposed to a UV and radiation environment. This embrittlement produced splits and cracks in the coverslide material upon undergoing thermal cycling representative of an orbital eclipse period. These cracks are probably a result of the highly stressed regions at the edges of the solar cell. A sprayed FEP process developed for JPL produces a coverslide with fewer stresses that may survive thermal cycling.

The projected values of mass per unit area for the developing thin solar cell arrays based on silicon, gallium arsenide and cadmium sulfide are strongly influence by the thickness requirements for the coverslide which basically provides protection against the radiation environment at GEO.

The "minimum" (pessimistic) solar cell efficiencies (air mass zero at 26°C) shown in Table 3.2 were based on today's values derived from data representing conventional (Helios) silicon solar cells (12%), available gallium arsenide cells (14%) and data for cadmium sulfide cells recently developed at the University of Delaware (8%). There is a significant difference between the confidence level established for the efficiency of silicon cells, now on orbit, and cadmium sulfide cells, for which a reasonable efficiency has only recently been attained. These data were included in the pessimistic category to represent the lower end of the range of efficiency for the three solar cell efficiencies being considered for the SSPS.

The "most likely" values of solar cell efficiency as shown in Table 3.2 are representative of the Comsat Non-Reflecting silicon cell (at normal incidence) (16%), recently attained values for gallium arsenide cells by IBM and Hughes Research Laboratories (18%) and near term projection by the University of Delaware research team of the efficiency of a cadmium sulfide cell (10%). The "optimistic" values of assumed solar cell efficiencies represent reasonable estimates of what could be achieved in the future.

The ranges of assumed mass per unit area for the three solar array materials are shown in Table 3.3. Tables 3.5, 3.6, and 3.7 show a mass breakdown for the three representative cells.

The "most likely" and "minimum" mass per unit area for the silicon array represent a 100 μm and 50 μm solar cell respectively with a reduced thickness FEP coverslide and a Kapton substrate.

Table 3.5 Mass Breakdown of Current* Silicon Cell

Cell Component	Material	Thickness (μm)	Mass (g/cm^2)
AR Coating	Ta_2O_5	.055	4.8×10^{-5}
Coverglass	Corning 7940	150	3.3×10^{-2}
Anode	TiPdAg	5	5.3×10^{-4}
Cell (12 mil)	Si	300	7.3×10^{-2}
Cathode	Al	5	1.4×10^{-3}
Substrate	Kapton	50	7.1×10^{-3}
			1.15×10^{-1}

* Maximum Mass/Unit Area

Table 3.6 Mass Breakdown of GaAs Cell*

Cell Component	Material	Thickness (μm)	Mass (g/cm^2)
Coverglass	FEP	125	2.67×10^{-2}
Anode	AgZn	5	5.22×10^{-4}
P Material	$Ga_{0.4}Al_{0.6}As$	1	3.49×10^{-4}
N Material	GaAs	5	2.23×10^{-3}
Cathode	AuSn	5	6.26×10^{-3}
Substrate	Kapton	50	7.1×10^{-3}
			4.32×10^{-2}

* Most Likely Mass/Unit Area

Table 3.7 Mass Breakdown of CdS Cell *

Cell Component	Material	Thickness (μm)	Mass (g/cm^2)
Coverglass	SiO_2	25	6.5×10^{-3}
Anode	Cu	.2	1.3×10^{-4}
P Material	Cu_2S	.2	1.1×10^{-4}
N Material	CdS	2	9.6×10^{-4}
Cathode	Ag	.2	2.1×10^{-4}
Substrate	Kapton	50	7.1×10^{-3}
			1.49×10^{-2}

* Most Likely Mass/Unit Area

The assumed solar array costs expressed in Table 3.4 as a cos per unit area, were derived from data that were expressed as a cost per peak kilowatt of generated electricity at a specified efficiency of con version. These cost data were modified slightly to make the minimum cost per unit area exactly the same for all three materials to reflect a thin cell array technology that is dominated by the costs of fabrication of the array on a reliable, mass production basis and is, therefor insensitive to the particular photovoltaic material being utilized. Table 3.8 summarizes the cost per kW parameters utilized to develop the cost per km^2 for the three materials. It is worth noting that a higher efficiency cell which has the same cost/kW as a lower efficiency cell, has a higher cost/km^2 than does the lower efficiency cell.

Of the three cell parameters, efficiency, mass per unit area and cost per unit area, it is the cost per unit area that has the largest percentage uncertainty associated with its 1990 projected value. The determination of the fabrication cost for square kilometers of an array which uses solar cells that are in an early stage of development was, therefore, based upon what were considered to be reasonable values for a cost per peak kilowatt of generated electricity and these cost numbers were then discussed with various photovoltaic investigators to obtain their opinions.

3.1.2.2 Optical System Configuration

To model the solar energy conversion subsystem of the SSPS over a range of concentration ratios required a definition for the geometry of the optical system at each level of concentration. It was also advantageous, from a subsystem modeling viewpoint, that the optical system's size and mass change smoothly as the degree of concentration was continuously varied. Figure 3.2 shows the wide range of optical configurations that have been proposed for the SSPS and Figure 3.3 shows seven simplified optical configurations that were extracted from the proposed configurations. Table 3.9 summarizes the three optical configurations used in the analyses. These three configurations were chosen because, of the seven candidates considered, they required the minimum area of optical surface reflector for each concentration ratio. An optimization study not performed in these analyses would be to tradeoff the decrease in cell efficiency for off-normal incidence sun angles using minimum mirror areas, against the additional mirror area needed to provide the same concentration ratio but with more normal incident angles to the solar cell (fewer but larger mirrors). These subsystem level analyses did consider the change in solar cell efficiency as a function of angle of incidence of arriving solar energy; however, only minimum area optical reflectors were utilized.

Table 3.8 Minimum, Most Likely, and Maximum Cost ($/kW) of Candidate Photovoltaic Solar Arrays at Stated Efficiencies

Solar Cell Material	Minimum	Most Likely	Maximum
Silicon	$257/kW (14%)	$457/kW (14%)	$3,000/kW (18%)
Gallium Arsenide	$300/kW (12%)	$1,000/kW (15%)	$5,000/kW (22%)
Cadmium Sulfide	$450/kW (8%)	$800/kW (8%)	$2,000/kW (10%)

PROPOSED CONFIGURATIONS	COMMENTS
1 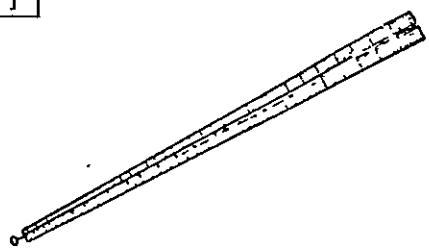	THE AEROSPACE CORPORATION • CABLE CONNECTED SEGMENTED SOLAR ARRAY • GRAVITY GRADIENT STABILIZATION • CONCENTRATION ≤ 1.0 • 58 KM LONG - LONG POWER DISTRIBUTION SYSTEM
2 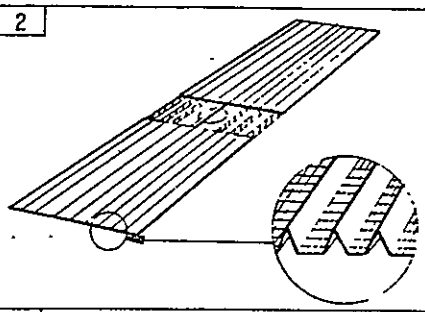	GRUMMAN / ADL / RAYTHEON / SPECTROLAB • PLANAR ARRAY WITH MIRROR TROUGHS 13.1 KM x 4.9 KM • CONCENTRATION < 3 WITH PLANAR MIRRORS • SEQUENTIAL OR PARALLEL FABRICATION OF STRUCTURE • DIELECTRIC STRUCTURE SURROUNDING MICROWAVE ANTENNA
3 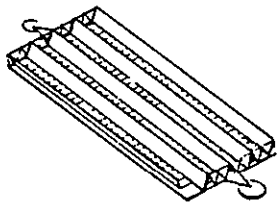	LYNDON B. JOHNSON SPACE CENTER • SAME AS CONFIGURATION NO. 2 EXCEPT MICROWAVE ANTENNAS ARE PLACED TO ELIMINATE NEED FOR DIELECTRIC STRUCTURE • CONCENTRATION < 3 WITH PLANAR MIRRORS • TWO ANTENNAS BALANCE MICROWAVE FORCES
4 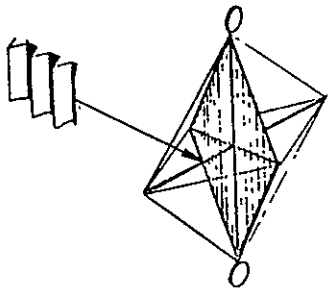	LYNDON B. JOHNSON SPACE CENTER • COLUMN/GUY WIRE STRUCTURE FOR LIGHTER STRUCTURE • SEQUENTIAL CONSTRUCTION NECESSARY • CONCENTRATION < 3 WITH PLANAR MIRRORS • TWO ANTENNAS BALANCE MICROWAVE FORCES
5 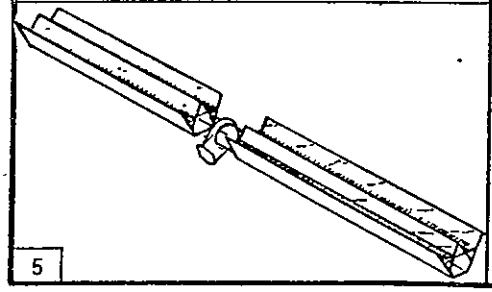	ROCKWELL INTERNATIONAL • HIGH ASPECT RATIO CONFIGURATION 25.5 KM x 2.0 KM • COMPATIBLE WITH CONTINUOUS FABRICATION STRUCTURE • CONCENTRATION < 3 WITH PLANAR MIRRORS • SINGLE STRUCTURAL ELEMENTS WITH CENTER ANTENNA ELIMINATES NEED FOR DIELECTRIC STRUCTURE

FIGURE 3.2 PROPOSED SSPS CONFIGURATIONS

PROPOSED CONFIGURATIONS	COMMENTS
11 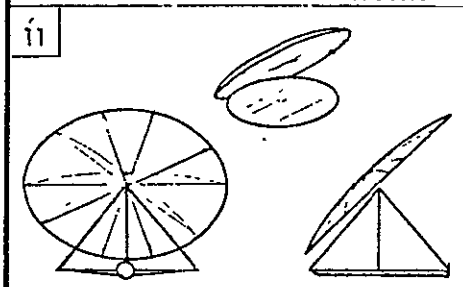	BOEING AEROSPACE COMPANY • SINGLE REFLECTING SURFACE ACTIVELY POSITIONED TO ILLUMINATE SOLAR ARRAY • NO ROTARY POWER JOINT REQUIRED
12 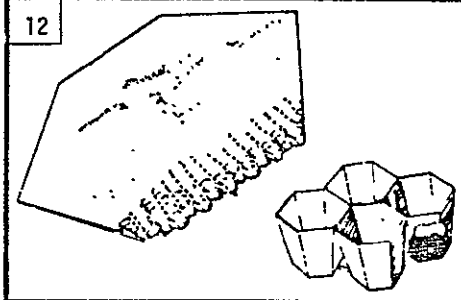	MOSES • HIGH DEGREE OF MODULARITY • HIGH POINTING ACCURACY REQUIRED • CONCENTRATION < 7 • PACKING FACTOR < 1 FOR UNIFORM ILLUMINATION OF ARRAY
13 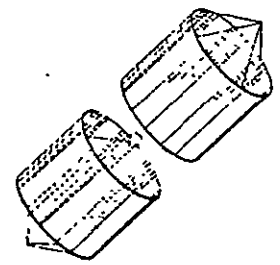	GRUMMAN • EARLY CURVED ARRAY CONCEPT TO PROVIDE A MORE UNIFORM GENERATION OF POWER WITH VARYING SUN ANGLE • CONCENTRATION < 1
14 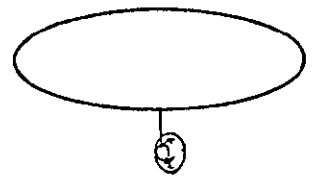	ADL • EARLY PLANAR DESIGN CONCEPT WITH REMOTELY SITUATED MICROWAVE ANTENNA • CONCENTRATION < 1
15 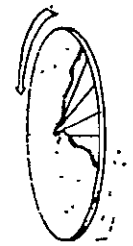	ADL • ROTATING STRUCTURE FOR TENSION STIFFENING OF ARRAY • CONCENTRATION < 1 • SUITABLE FOR LARGE LIGHTWEIGHT ARRAY USED WITH A LOW COST AND RELATIVELY INEFFICIENT PHOTO-VOLTAIC MATERIAL • NO OPTICS

FIGURE 3.2 (Continued)

PROPOSED CONFIGURATIONS	COMMENTS
6 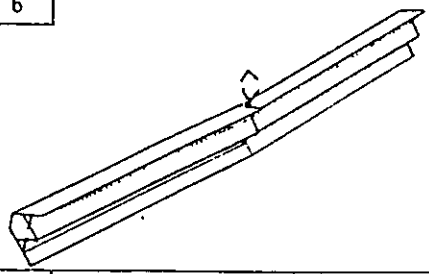	ROCKWELL INTERNATIONAL • SAME CONCEPT AS NO. 5 EXCEPT A 5° CANT ANGLE WITH MICROWAVE ANTENNA ABOVE SOLAR ARRAY • INCLUSION OF 5° CANT ANGLE TO REDUCE GRAVITY GRADIENT TORQUE AND PROPELLANT CONSUMPTION HAS SMALL EFFECT ON ARRAY COLLECTION EFFICIENCY • CONCENTRATION < 3 WITH PLANAR MIRRORS
7 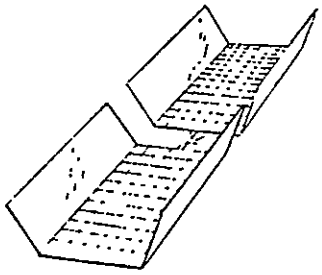	• SINGLE TROUGH CONCEPT • CONCENTRATION < 3 • DIFFICULT TO PROVIDE ACTIVE COOLING OF SOLAR ARRAY • DIFFICULT TO FABRICATE LARGE LIGHTWEIGHT REFLECTING OPTICS WITH PLANAR SURFACES
8 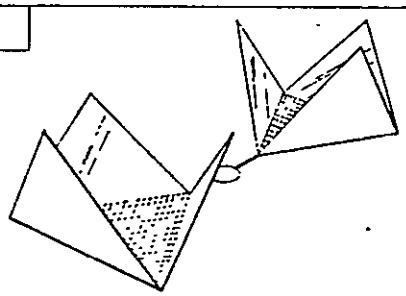	BOEING AEROSPACE COMPANY • CONCENTRATION < 4 WITH 2 AXES POINTING • DIFFICULT TO PROVIDE ACTIVE COOLING OF SOLAR ARRAY • DIFFICULT TO FABRICATE LARGE LIGHTWEIGHT REFLECTING OPTICS WITH PLANAR SURFACES
9 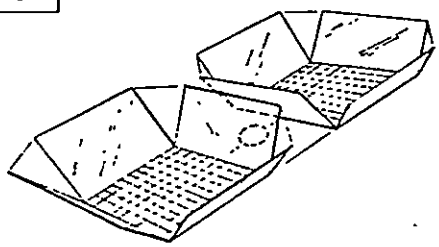	• CONCENTRATION < 5 WITH 2 AXES POINTING • DIFFICULT TO PROVIDE ACTIVE COOLING OF SOLAR ARRAY • DIFFICULT TO FABRICATE LARGE LIGHTWEIGHT REFLECTING OPTICS WITH PLANAR SURFACES • PACKING FACTOR < 1
10 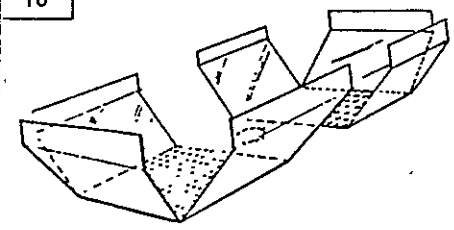	• CONCENTRATION < 7 WITH 2 AXES POINTING • PACKING FACTOR < 1

FIGURE 3.2 (Continued)

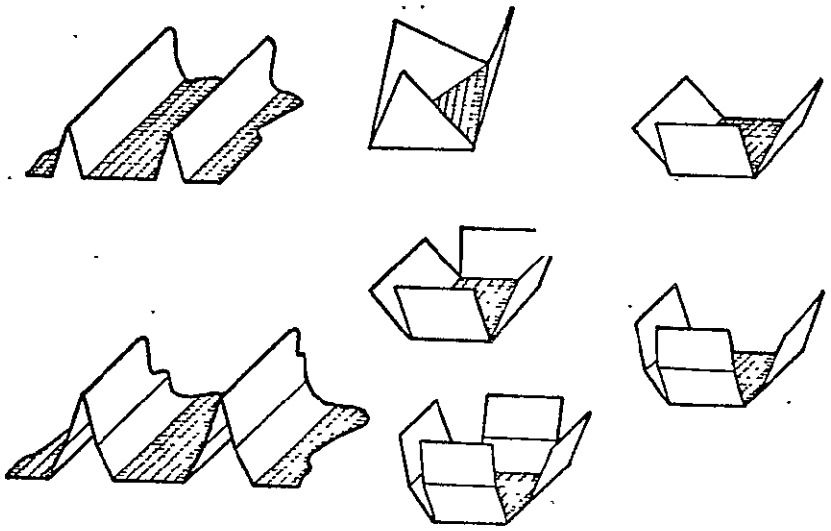

FIGURE 3.3 SIMPLIFIED OPTICAL CONFIGURATIONS CONSIDERED FOR THIS TASK

Table 3.9 Optical Configurations Used in Analyses

C.R. = 1.0	
1.0 < C.R. $\leq$ 3.8	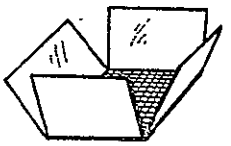
3.8 < C.R.	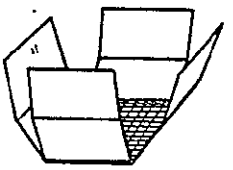

3.1.2.3 Cooling System Options

Because solar cell conversion efficiency decreases with increasing temperature, it is desirable to operate the illuminated solar cells at as low a temperature as possible. The basic options available to decrease the temperature of an operating cell are: (1) reduce the amount of absorbed solar energy that is not being efficiently converted to electrical energy by the cell through the use of selective coatings on the optics or on the cell, (2) enhance the IR emittance of the cell/array front and back surfaces and (3) thermally couple the solar array area to a larger radiating area, through the use of a conducting substrate and/or a heat pipe or liquid (gas) loop cooling system.

In order to reduce the complexities and uncertainties of the SSPS design and of the comparative analyses of alternative solar cell materials, no augmented cooling schemes or selective filtering techniques were used in the model of the solar energy conversion subsystem. This assumption reduces the optimum concentration ratio for each of the cell materials because of the increase in cell temperature, resulting in a decrease in conversion efficiency, as the concentration ratio is increased. Of the three materials, gallium arsenide is affected least by this assumption because of its smaller change in conversion efficiency as a function of temperature (see Table 3.10).

Table 3.10 Temperature Coefficient of Conversion Efficiency for Three Candidate Solar Cell Materials

Solar Cell Material	Temperature Coefficient of Conversion Efficiency (%/°C)
Silicon	-0.055
Cadmium Sulfide	-0.036
Gallium Arsenide	-0.024

4. RESULTS OF ENERGY CONVERSION SYSTEM STUDIES

The relative ranking of the different materials based upon a comparison of the "parametric cost" as developed in this subsystem level analysis is dictated by the current and projected values of the solar cell characteristic properties of efficiency, mass per unit area and cost per unit area. These three parameters are part of a larger set of parameters that define the full SSPS system, and it is ultimately a system level decision as to which solar cell material is optimum for the SSPS.

The results presented show three relative rankings for the three different solar cells as a function of concentration ratio. These rankings are based upon three different sets of assumptions which define, basically, the solar cell mass and cost per unit area. In addition, the variation in parametric cost has also been computed as a function of variations in specific properties of a solar cell.

4.1 Definition of Parametric Cost and Mass Parameters

The results of the subsystem level analyses of alternative solar cell materials were summarized into a single output parameter, a parametric cost per kilowatt of generated electricity at the utility interface. The term parametric cost is used to distinguish the output from these subsystem level analyses from the full system level cost results which considered many additional cost factors. The parametric cost, as defined in these deterministic analyses, specifically includes the following items:

1. capital cost of solar cell array,
2. capital cost of optical reflectors,
3. capital cost of basic supporting structure,
4. total mass of solar cell array, optical reflectors and basic support structure multiplied times the transportation cost to GEO per unit mass.

A fixed 5 GW delivered to the utility interface at a specified point in the lifetime of the SSPS (5 years for these analyses) was used as the denominator to compute "parametric cost" ($/kW). The parametric cost was not discounted.

The subsystem mass computed in these analyses consisted of the mass of the solar cell array, the optical reflectors and the basic support structure.

4.2 Parametric Cost Results for Selected Photovoltaic Materials

Figure 4.1 shows the computed parametric cost as a function of concentration ratio for the three different photovoltaic materials using "most likely" values for the parameters which characterize the solar cell array. Figures 4.2 (Case I) and 4.3 (Case II) show the computed "parametric cost" as a function of concentration ratio for the three different photovoltaic materials for different assumed values for the solar array parameters. The assumptions inherent in these two different sets of data are summarized in Table 4.1. Basically, Case I compares a current 300 μm silicon cell having a 150 μm coverslide with a 5 μm gallium arsenide cell with its 125 μm coverslide and a 2 μm cadmium sulfide cell with a 25 μm coverslide. Case II compares a 50 μm silicon cell having a 150 μm coverslide with a 10 μm gallium arsenide cell and a 5 μm cadmium sulfide cell both having a 50 μm coverslide. "Most likely" cost numbers were used in Case I and "minimum" cost numbers were utilized in Case II.

The purpose of displaying these sets of data is to show the different conclusions that can be drawn regarding the photovoltaic subsystem of the SSPS based upon which set of cell parameters were utilized in the analyses. It is recognized that it is not necessary to make a choice today as to which type of photovoltaic material should be utilized for the SSPS particularly in view of the significant advances being made. What is most important is to continue to develop potentially promising candidate materials and to pursue a reduction in the uncertainties in projected cell performance, mass and, especially, cost parameters. The emerging solar cell technology should be continuously monitored to establish which solar cell candidates promise to offer the set of characteristics which are optimum for the SSPS. Desirable characteristics of high efficiency, low mass and low cost represent general development goals for the solar energy conversion system.

An additional result from the analyses of the solar energy conversion subsystem is the total projected area of the SSPS as a function of concentration ratio for the three different photovoltaic materials as shown in Figure 4.4. Without augmented cooling, an increase in concentrating ratio results in an increase in solar cell temperature and a decrease in the conversion efficiency of the subsystem. A reduction in conversion efficiency results in the need for additional solar radiation to be intercepted and, therefore, the total area of the SSPS increases. An important system level trade not incorporated into the present analyses is a comparison of the cost to construct an additional square kilometer of basic SSPS structure and the cost savings achieved by a reduction in the area of solar cell array, both of which would occur with an increase in concentration ratio with no augmented cooling.

Figures 4.1 through 4.3 have shown that at a subsystem level and for concentration ratios greater than three, a gallium arsenide solar cell array has the lowest parametric cost. By repeating the Case I set of assumptions, except that "maximum" array costs are used instead of

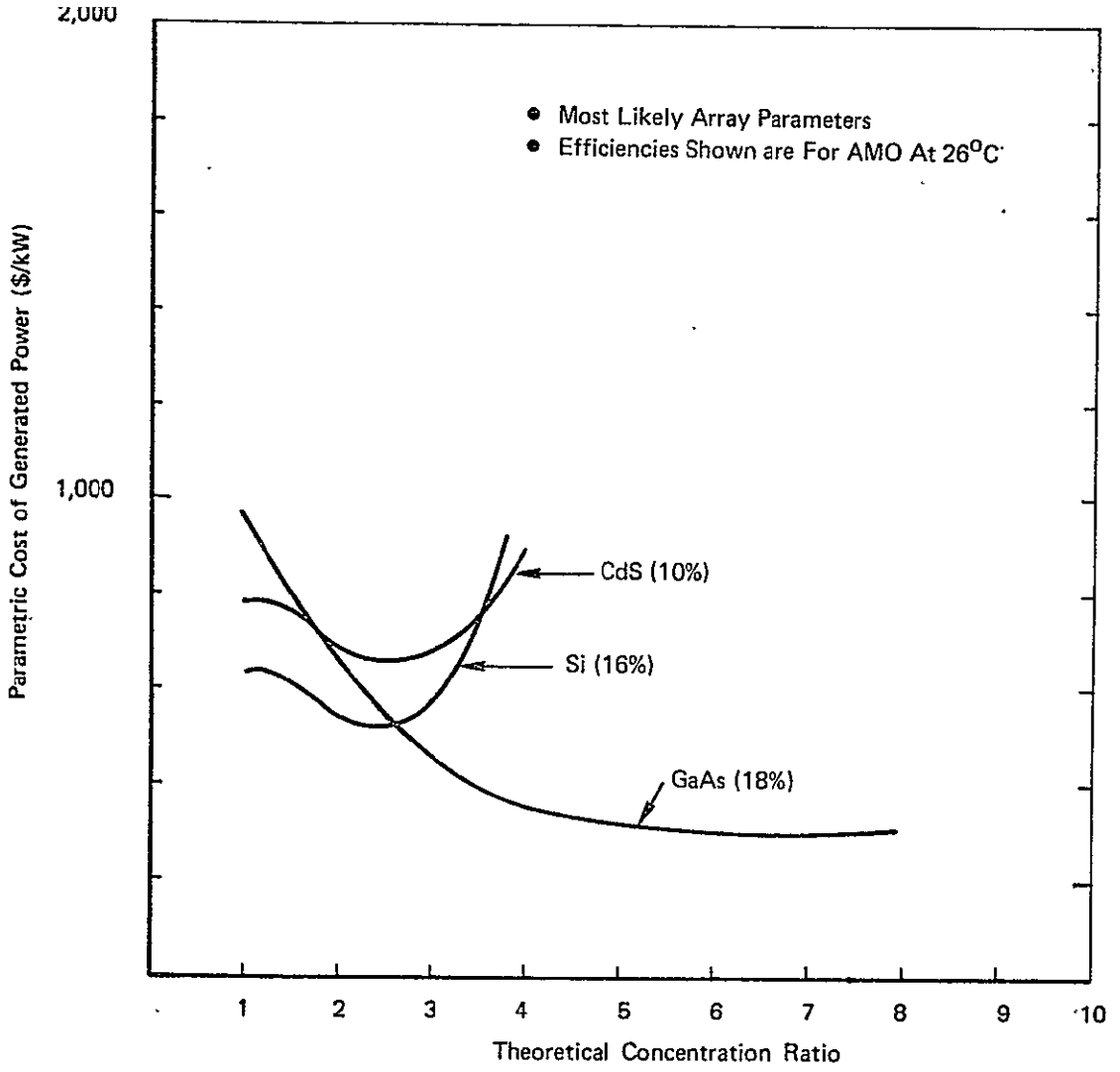

FIGURE 4.1 VARIATION IN PARAMETRIC COST OF 5GW OF GENERATED POWER AS A FUNCTION OF CONCENTRATION RATIO FOR THREE DIFFERENT SOLAR CELL MATERIALS MOST LIKELY PARAMETERS

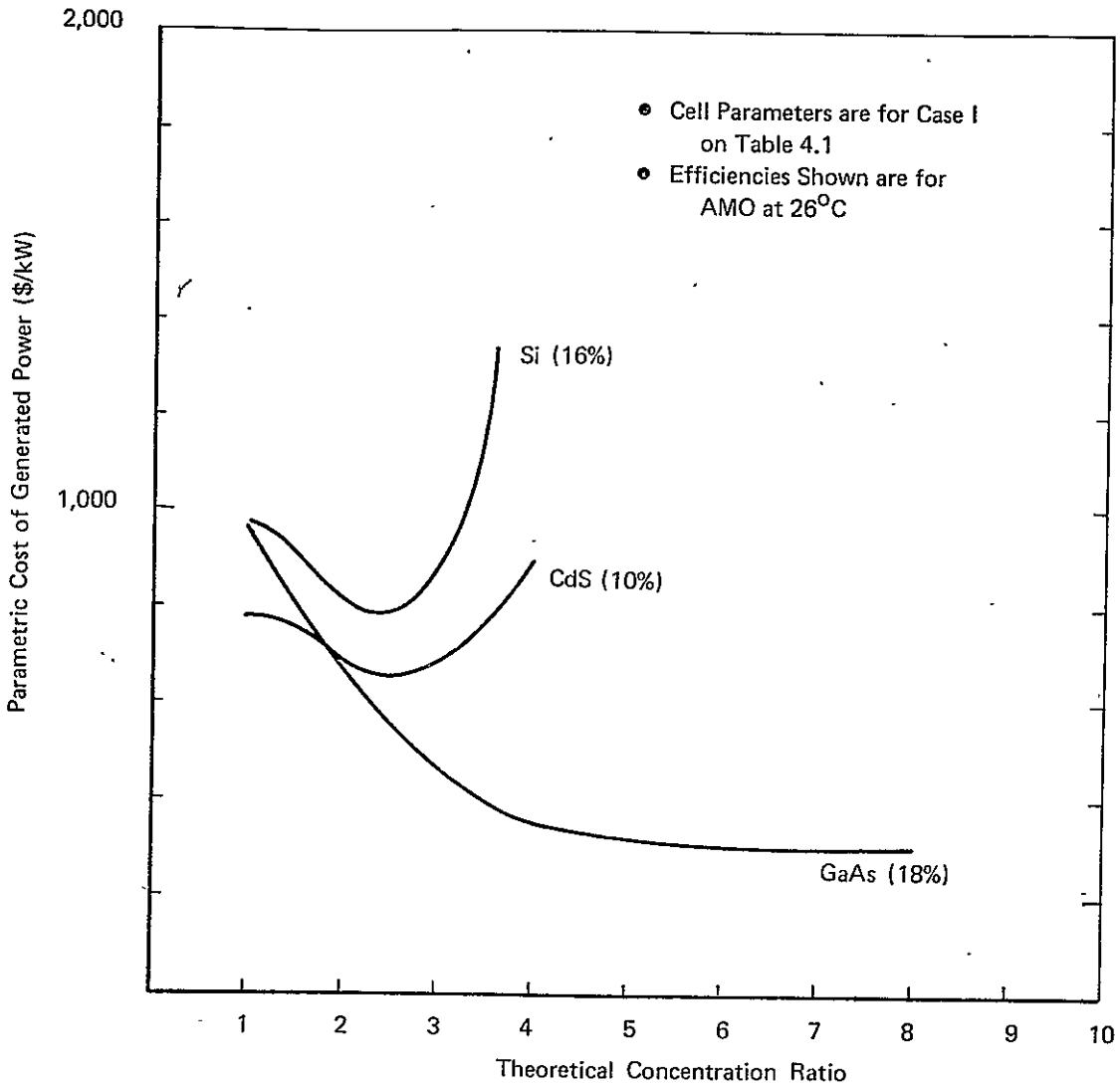

FIGURE 4.2 VARIATION IN PARAMETRIC COST OF GENERATED POWER ($/kW) AS A FUNCTION OF CONCENTRATION RATIO FOR THREE DIFFERENT SOLAR CELL MATERIALS – I

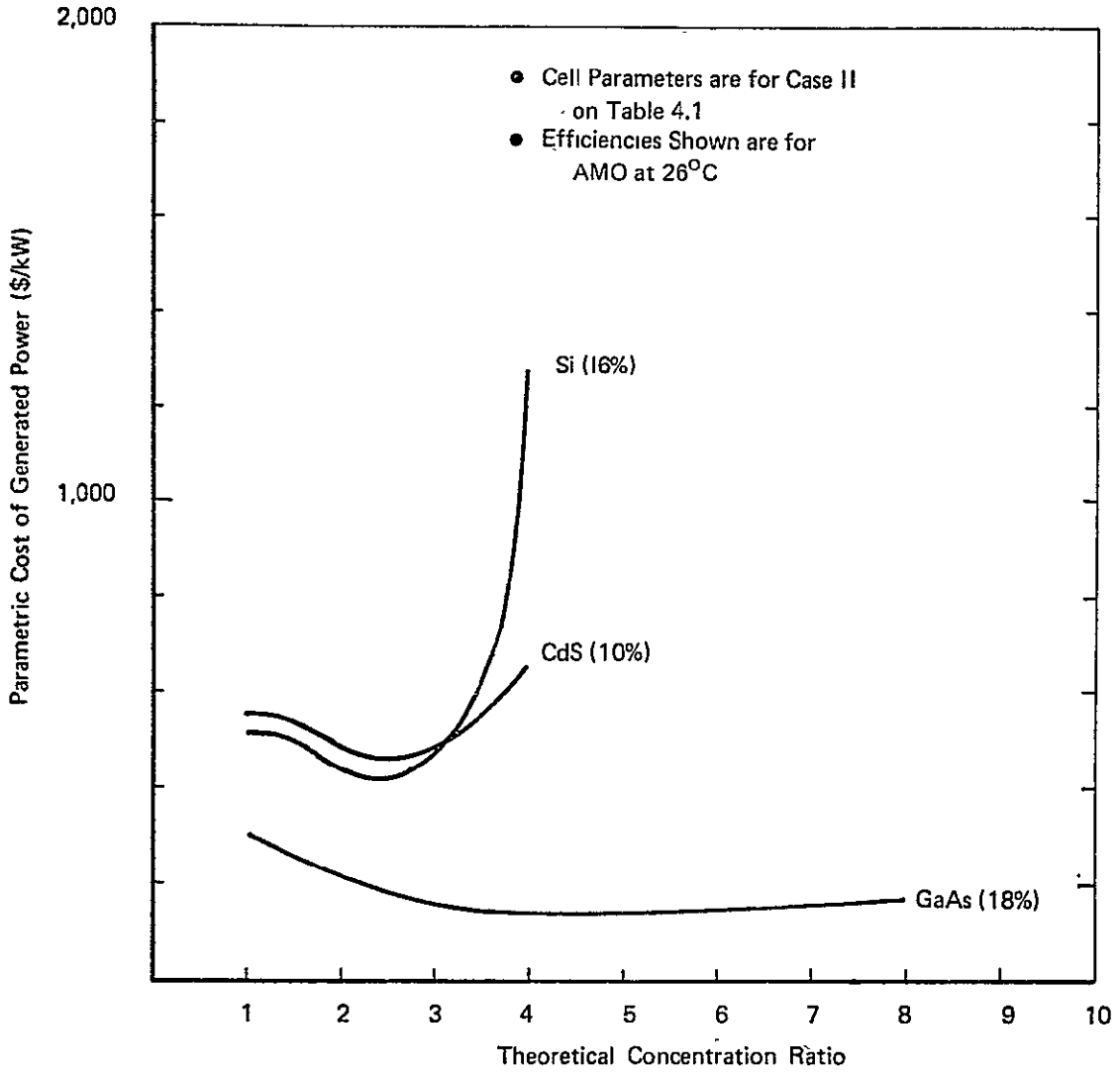

FIGURE 4.3 VARIATION IN PARAMETRIC COST OF GENERATED POWER ($/kW) AS A FUNCTION OF CONCENTRATION RATIO FOR THREE DIFFERENT SOLAR CELL MATERIALS – II

Table 4.1 Summary of Deterministic Assumptions Inherent in Comparison Analyses of Three Different Solar Cell Materials in Cases I and II

Parameter	Solar Cell Material					
	Si		GaAs		CdS	
	I	II	I	II	I	II
Cover Thickness (μm)	150	150	125	50	25	50
Cell Thickness (μm)	300	50	5	10	2	5
Cell Mass/Unit Area (mg/cm^2)	115.	60.6	43.2	36.1	14.9	27.2
Cell Cost/Unit Area ($\$10^6/km^2$)	86.6	48.7	203	48.7	86.6	48.7
Conversion Efficiency (%) AMO 26°C	16	16	18	18	10	10

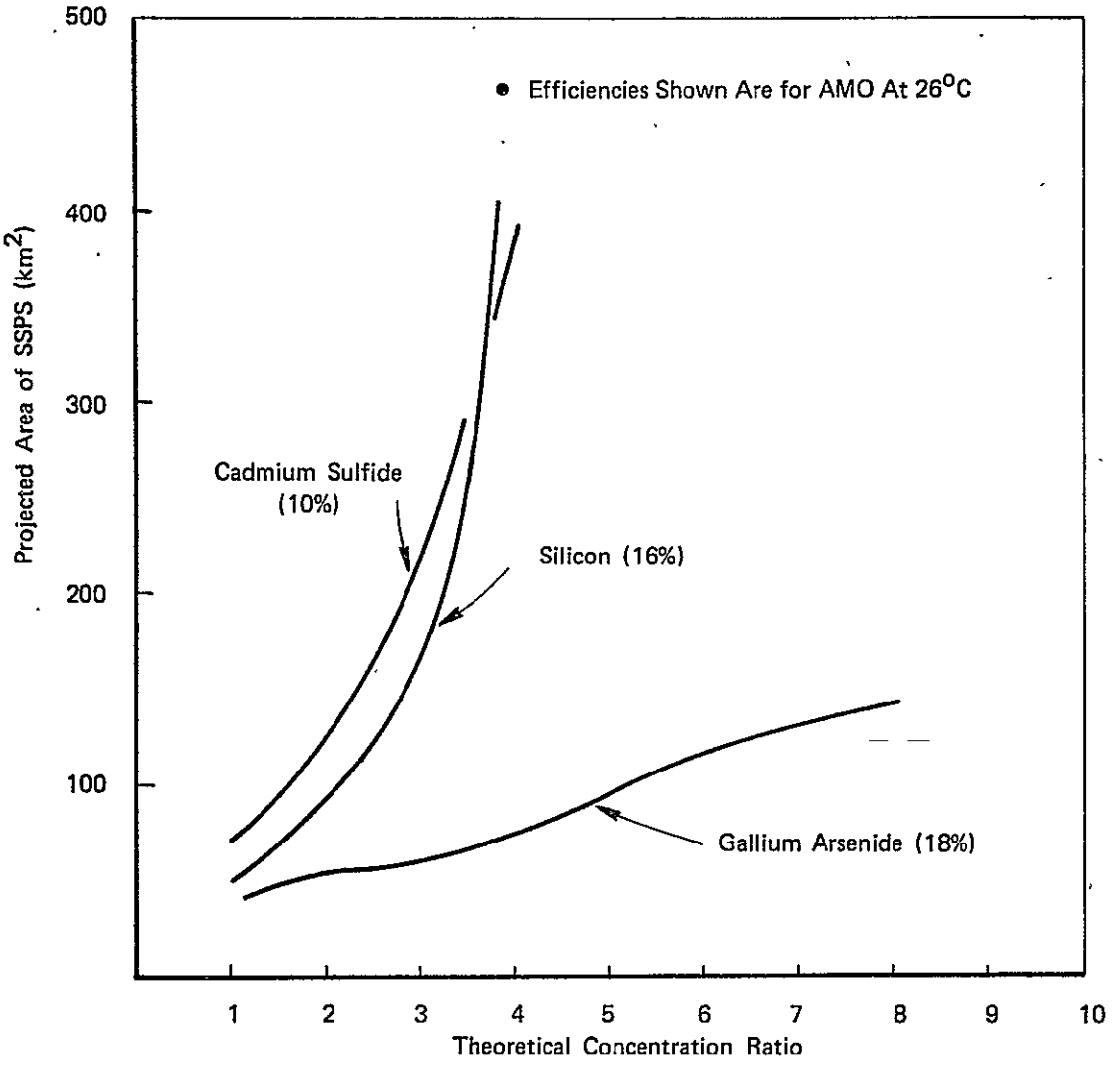

FIGURE 4.4 VARIATION IN TOTAL PROJECTED AREA (km^2) OF SSPS AS A FUNCTION OF CONCENTRATION RATIO FOR THREE DIFFERENT SOLAR CELL MATERIALS

"most likely" values, cadmium sulfide becomes the cell material having the lowest computed parametric cost up to a concentration ratio of approximately 4.0. These results are shown in Figure 4.5.

The significance of these results is that if a deterministic comparative analysis of alternative solar cell materials for the SSPS is performed in which specific values are assigned to each parameter, chosen from its range of uncertainty, then the comparative parametric costs of the alternative cell materials is determined by the logic which was utilized to select each parameter from its range of uncertainty. A large range of uncertainty in a particular parameter can produce a significant variation in the relationship between the parametric costs of the alternative cell materials. This is the example demonstrated in Figure 4.5 for the projected "maximum" cost of a gallium arsenide solar cell array. As is the case for the system level analyses of the SSPS performed by ECON, a probability distribution for the parameters of performance, mass per unit area and cost per unit area for the solar cell array, should be included in any comparative analysis of alternative solar cell materials at the subsystem level. Then, the deterministic model of the energy conversion subsystem can be exercised in a stochastic sense to yield probability distributions that describe the uncertainty associated with a particular analysis of alternative solar cell materials. This analytical approach provides at the subsystem level (as it does for the full system level analyses) a procedure for evaluating the effect on the relationship between the parametric costs of the candidate cell materials caused by a reduction in the uncertainty of one or more solar cell parameters.

The concept of concentrating solar radiation with the solar energy conversion subsystem is the result of a desire to minimize the amount of solar cell array needed to produce a given output of electrical power, i.e., to maximize the electrical power produced per unit area of array. The solar array represents a significant fraction of the materials cost and mass of the total SSPS, and a reduction in the required area of the solar cell array could reduce several obvious cost factors of the SSPS. However, it would be necessary to include the cost, with associated uncertainties, for construction of both a unit area of the basic support structure and also of the optical reflector system, as well as the cost and uncertainties associated with installing the solar cell array, to obtain realistic system level trade analyses for judging the relative merits of concentration vs. no concentration. Simpler structural design approaches can be considered if no concentration is utilized.

Figures 4.6 through 4.10 show the computed variation in mass of the solar cell array and of the combined mass of the optics and support structure as a function of concentration ratio, for the three different cell materials. Because of the large uncertainty in the projected mass of the silicon cell array that was analyzed, results from both a heavy (115 mg/cm^2) and light (28.2 mg/cm^2) silicon cell array are shown. Figure 4.6 shows the variation in parametric cost of generated power as a function of concentration ratio and array density for a silicon solar cell array. Figures 4.7 and 4.8 show, as bar graphs, the mass of the array and the

combined mass of the optics and support structure, for high and low mass silicon cell arrays. Figures 4.9 and 4.10 present the results for gallium arsenide and cadmium sulfide. The significance of these plots is that, with the exception of gallium arsenide, the reduction in array mass (area) is not as significant as is the increase in mass (area) of the optical reflector and basic support structure. This result is caused by the assumption of no augmented cooling so that cell temperature rises and cell efficiency decreases with increasing concentration, thereby causing the overall size of the SSPS to increase (Figure 4.4).

Additional parametric runs were made with the solar energy conversion subsystem computer model and Figures 4.11, 4.12, and 4.13 show the variation in parametric cost as a function of concentration ratio for the three different materials and includes the assumed range of basic cell efficiency. The significance of these runs is that the concentration ratio at minimum parametric cost does not appear to be a significant function of solar cell efficiency.

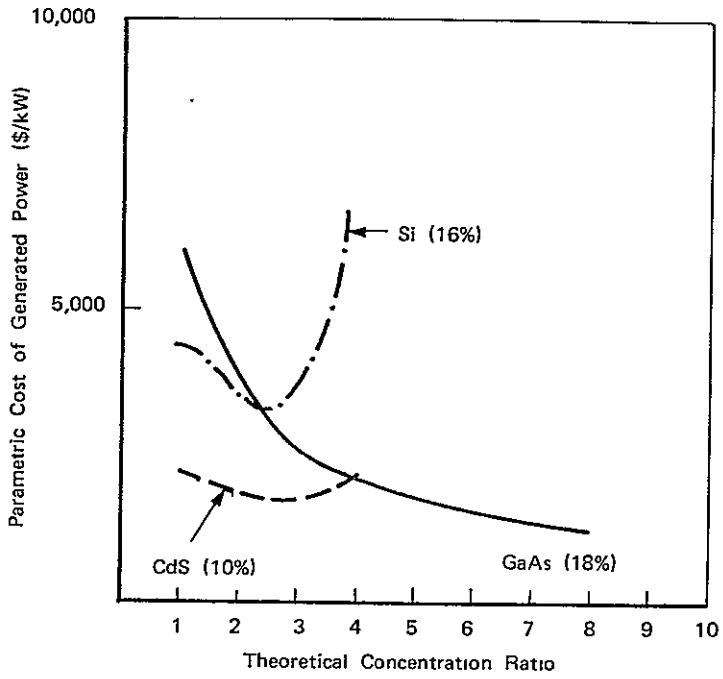

FIGURE 4.5 VARIATION IN PARAMETRIC COST OF GENERATED POWER ($/kW) AS A FUNCTION OF CONCENTRATION RATIO FOR THREE DIFFERENT SOLAR CELL MATERIALS – MAXIMUM ARRAY COSTS

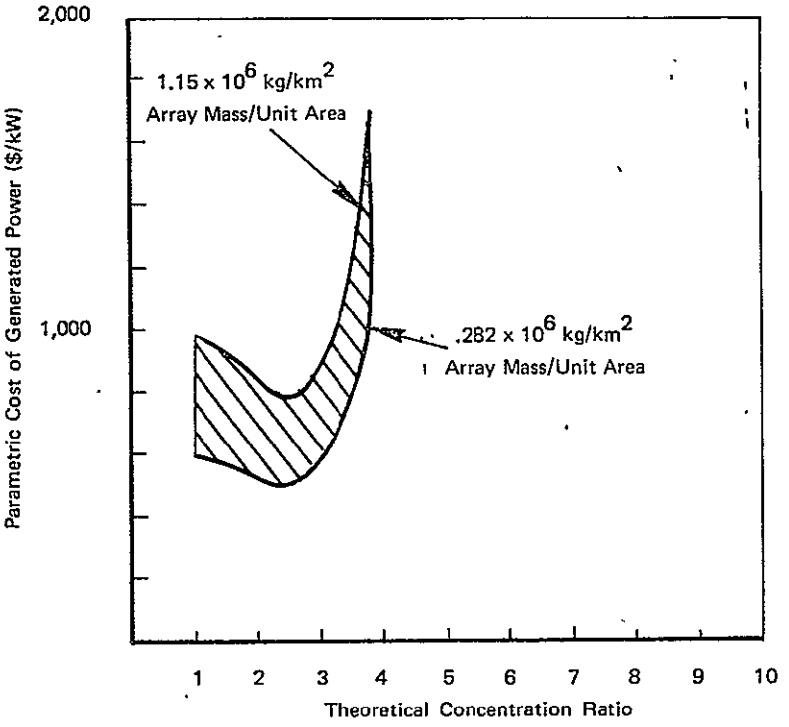

FIGURE 4.6 VARIATION IN PARAMETRIC COST OF GENERATED POWER ($/kW) AS A FUNCTION OF CONCENTRATION RATIO FOR DIFFERENT DENSITIES OF SILICON ARRAY (16% EFFICIENT CELL AT AMO AND 26°C)

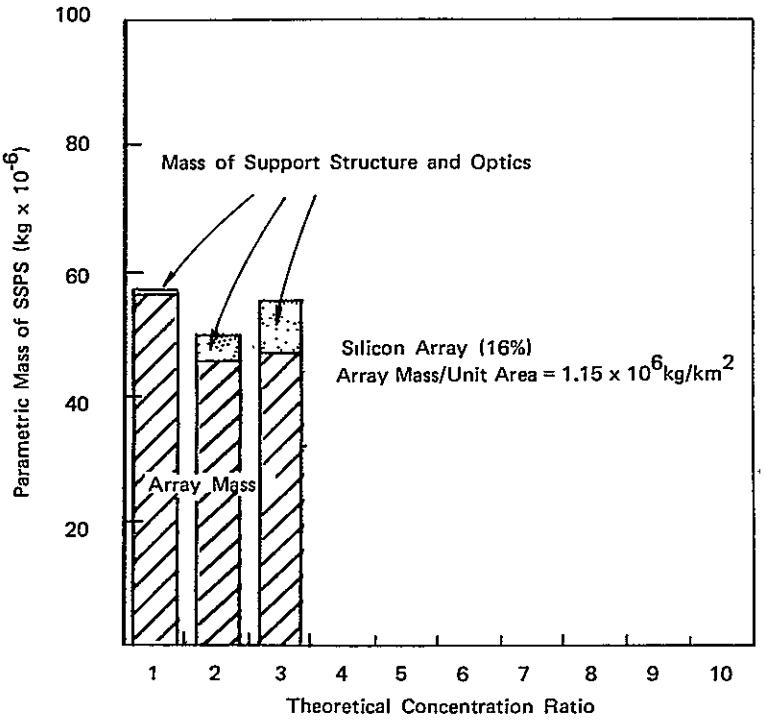

FIGURE 4.7 VARIATION IN PARAMETRIC MASS OF SSPS (kg x 10^{-6}) AS A FUNCTION OF CONCENTRATION RATIO FOR A SILICON CELL ARRAY (16%) MAXIMUM ARRAY MASS PER UNIT AREA

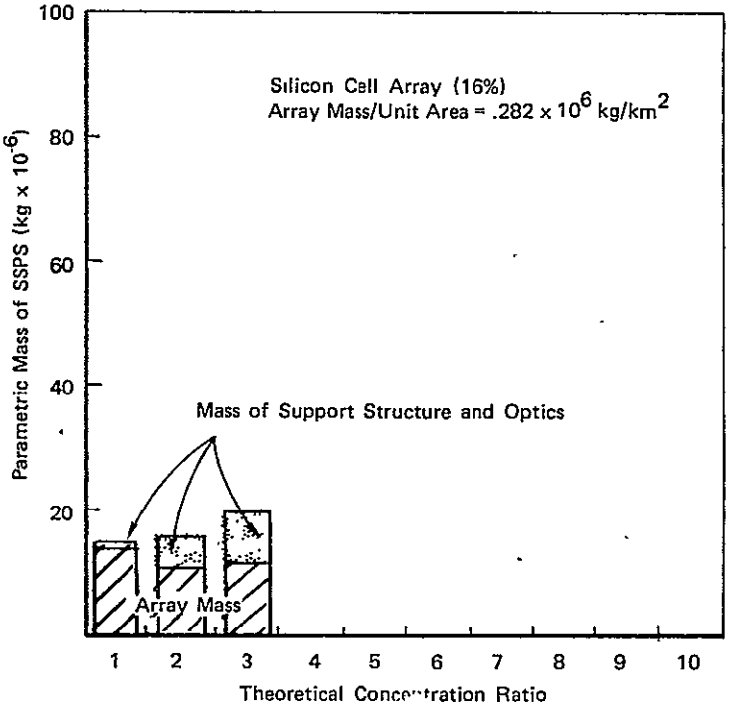

FIGURE 4.8 VARIATION IN PARAMETRIC MASS OF SSPS (kg x 10^{-6}) AS A FUNCTION OF CONCENTRATION RATIO FOR A SILICON CELL ARRAY (16%) MINIMUM ARRAY MASS PER UNIT AREA

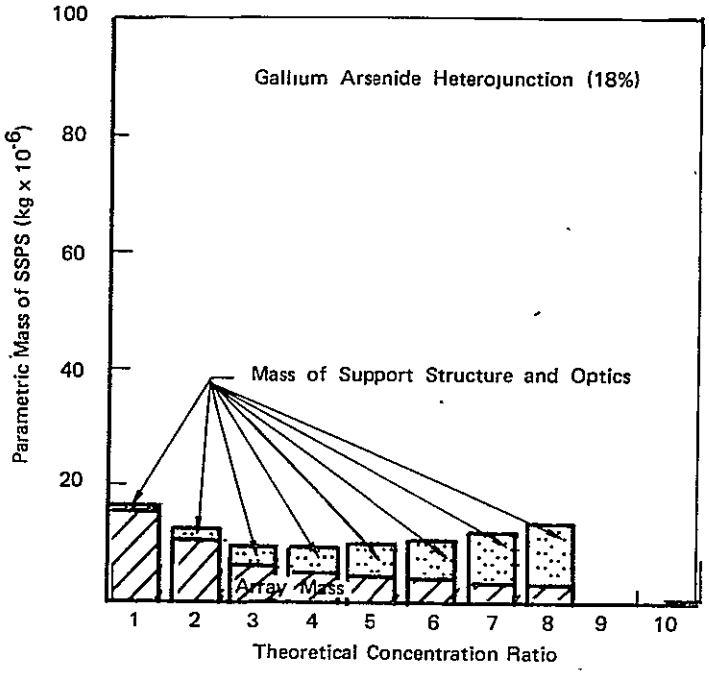

FIGURE 4.9 VARIATION IN PARAMETRIC MASS OF SSPS ($kg \times 10^{-6}$) AS A FUNCTION OF CONCENTRATION RATIO FOR A GALLIUM ARSENIDE HETEROJUNCTION (18%)

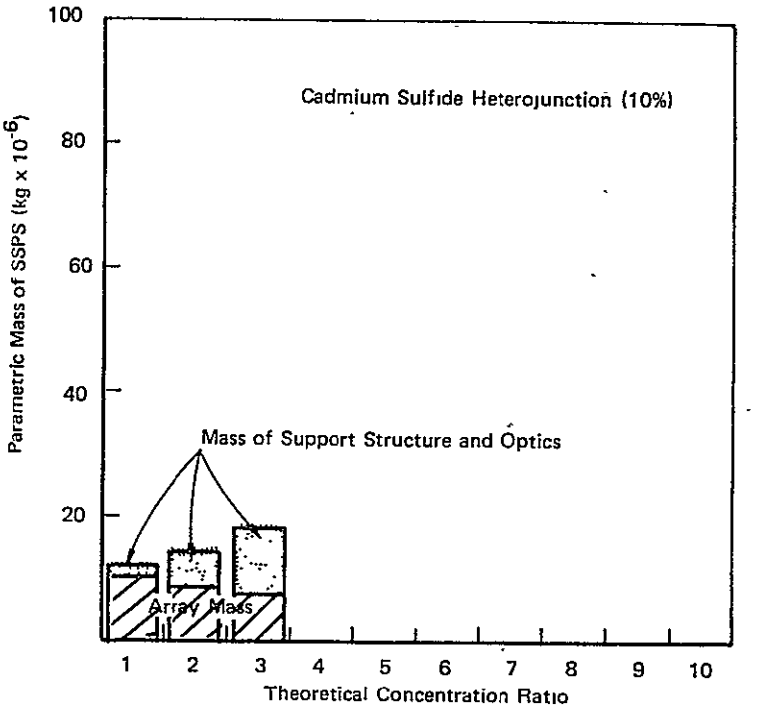

FIGURE 4.10 VARIATION IN PARAMETRIC MASS OF SSPS (kg x 10^{-6}) AS A FUNCTION OF CONCENTRATION RATIO FOR A CADMIUM SULFIDE CELL ARRAY (10%)

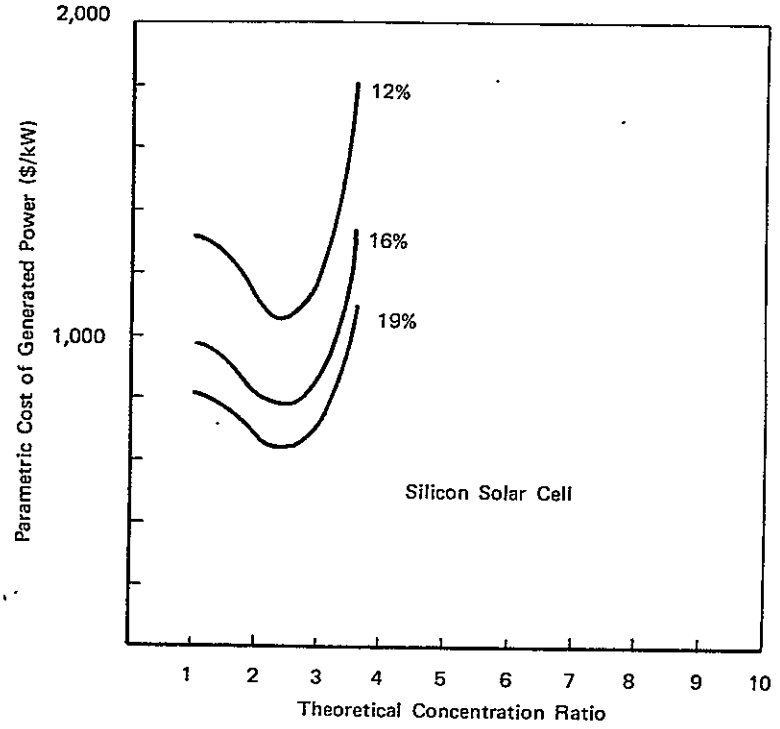

FIGURE 4.11 VARIATION IN PARAMETRIC COST OF GENERATED POWER ($/kW) AS A FUNCTION OF BASIC SOLAR CELL EFFICIENCY AND CONCENTRATION RATIO – SILICON

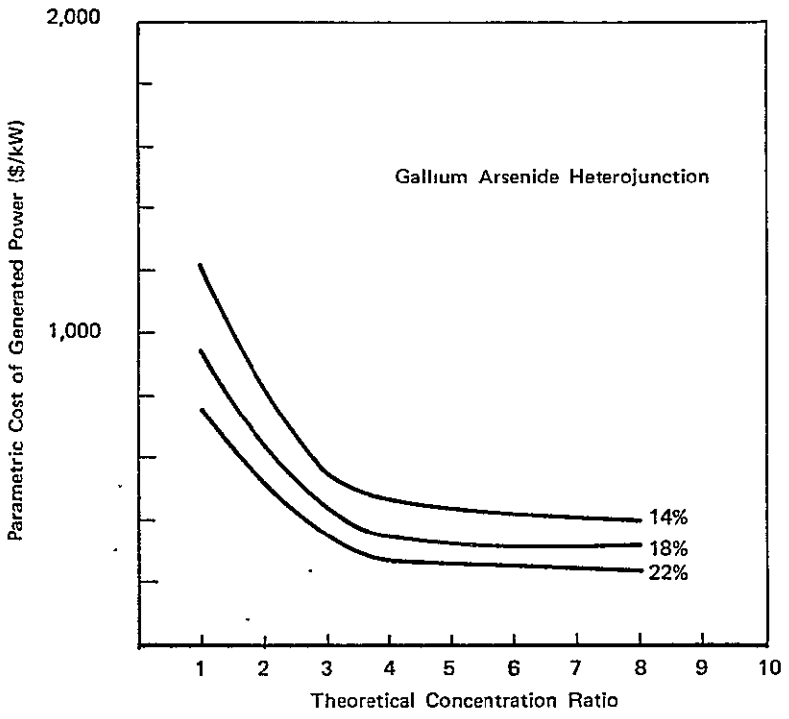

FIGURE 4.12 VARIATION IN PARAMETRIC COST OF GENERATED POWER ($/kW) AS A FUNCTION OF BASIC SOLAR CELL EFFICIENCY AND CONCENTRATION RATIO – GALLIUM ARSENIDE

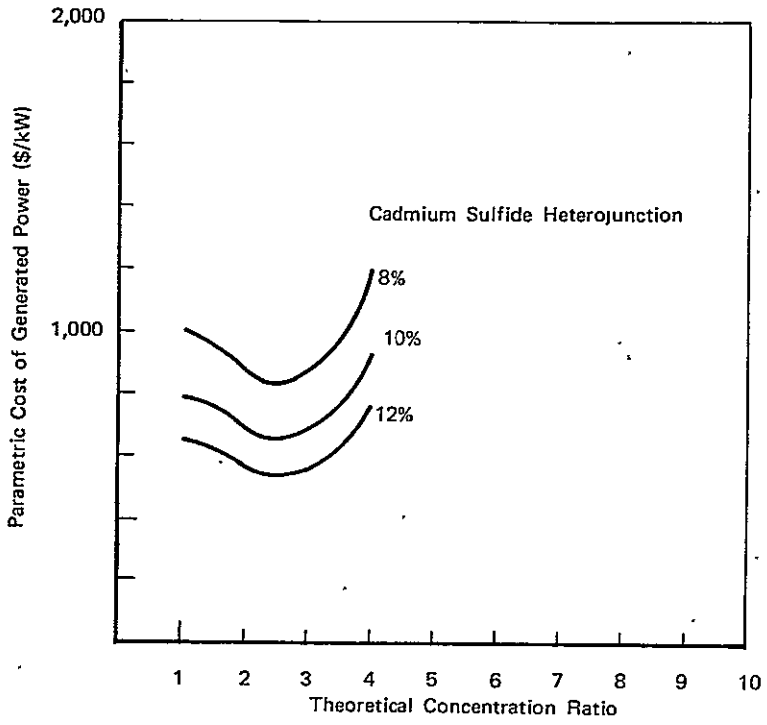

FIGURE 4.13 VARIATION IN PARAMETRIC COST OF GENERATED POWER ($/kW) AS A FUNCTION OF BASIC SOLAR CELL EFFICIENCY AND CONCENTRATION RATIO – CADMIUM SULFIDE

5. CONCLUSIONS

1. The state-of-the-art in solar cell technology is currently advancing at a very rapid rate such that any completed data bank representing available photovoltaic materials for the SSPS can only be of temporary validity.

2. Among the three photovoltaic materials which were examined at the solar energy conversion subsystem level, gallium arsenide would have the lowest parametric cost for systems at higher concentration ratios with no augmented cooling. For systems with low or no concentration and with no augmented cooling, the results of the deterministic, subsystem level analyses did not indicate a single photovoltaic material as having the minimum parametric cost. The relative merits of the three photovoltaic materials based on parametric cost, was dependent on the process for selecting specific cell parameters from their range of uncertainty.

The subsystem analyses show that a solar concentration ratio near 2.4 for silicon and cadmium sulfide and greater than 7.0 for gallium arsenide will minimize the computed parametric cost for these materials.

3. Optical concentrators and augmented cooling result in increasing complexity of the solar energy conversion system, tighter pointing requirements and an increased difficulty of fabrication and assembly in orbit. A reduced operational life due to degradation of reflecting surfaces may also result. These effects were not quantified in this task.

4. Increased concentration ratios will result in a reduction of the required total area of solar cell arrays but will reduce solar cell efficiency, without augmented cooling, because of higher cell equilibrium temperatures. This results in an increase in the total solar energy conversion system area. The increased costs of fabrication and assembly of the larger solar energy conversion system with optical concentration can drive the concentration ratio at which the parametric cost is minimum towards 1.0.

5. Solar energy conversion subsystem designs which utilize thin film solar cells without concentration and without augmented cooling can result in a simpler structural design, thereby reducing complexities of orbital fabrication and assembly at an acceptable performance. Lower mass system designs can produce a more competitive SSPS when compared to alternative energy production methods.

6. The SSPS analyzed configuration utilizing single crystal silicon solar cells with optical concentrators has performed a very useful function for technical and economic feasibility and system studies, but does not represent an optimum design approach. Future designs should examine evolving thin film solar cell technology and alternative structural approaches, which are more consistent with the projected low mass solar

cell arrays of the future and which lend themselves to less complex fabrication and assembly procedures in orbit.

7. A deterministic methodology has been developed to analyze the solar energy conversion subsystem characteristics. The limitation to this approach is that uncertainties in cell parameters cannot be adequately represented. To improve this methodology for subsystem level analyses, stochastic modeling of the uncertainties in the parameters should be employed.

6. RECOMMENDATIONS

1. The current data base on photovoltaic materials should be expanded to include other candidate solar cells, particularly those applicable to the SSPS solar energy conversion subsystem.

2. Uncertainties and inconsistencies in the properties and performance of photovoltaic materials and solar cells should be reduced through a standardization of test methods, so that photovoltaic material properties of different cells can be documented on a consistent basis. A stochastic model of the solar energy conversion subsystem should be utilized to assess the impact of uncertainties in current solar cell technology on the SSPS program.

3. The activities directed towards the development of photovoltaic materials for the SSPS should be coordinated with the development activities pertaining to terrestrial photovoltaic conversion applications, which includes efforts to standardize the test methods for solar cells.

4. The solar cell materials for which performance, production processes and costs show the most promise for applications to the SSPS solar energy conversion system should be investigated in greater detail so as to reduce the uncertainties in the projected cell parameters.

5. Orbital experimental tests should be conducted to verify on-orbit performance of promising photovoltaic materials to provide design data required for the solar energy conversion subsystem.

6. Figure 6.1 shows a recommended program scenario for the investigation and development of photovoltaic materials and solar array blankets for the SSPS over the time period from today to 1996.

7. SSPS designs based on thin film solar cells without concentration and utilizing new structural approaches should be developed and associated fabrication and assembly costs established for inclusion in system trade-off studies. The effects of station keeping and reduced pointing requirements on the attitude control system and its propellant consumption should be established.

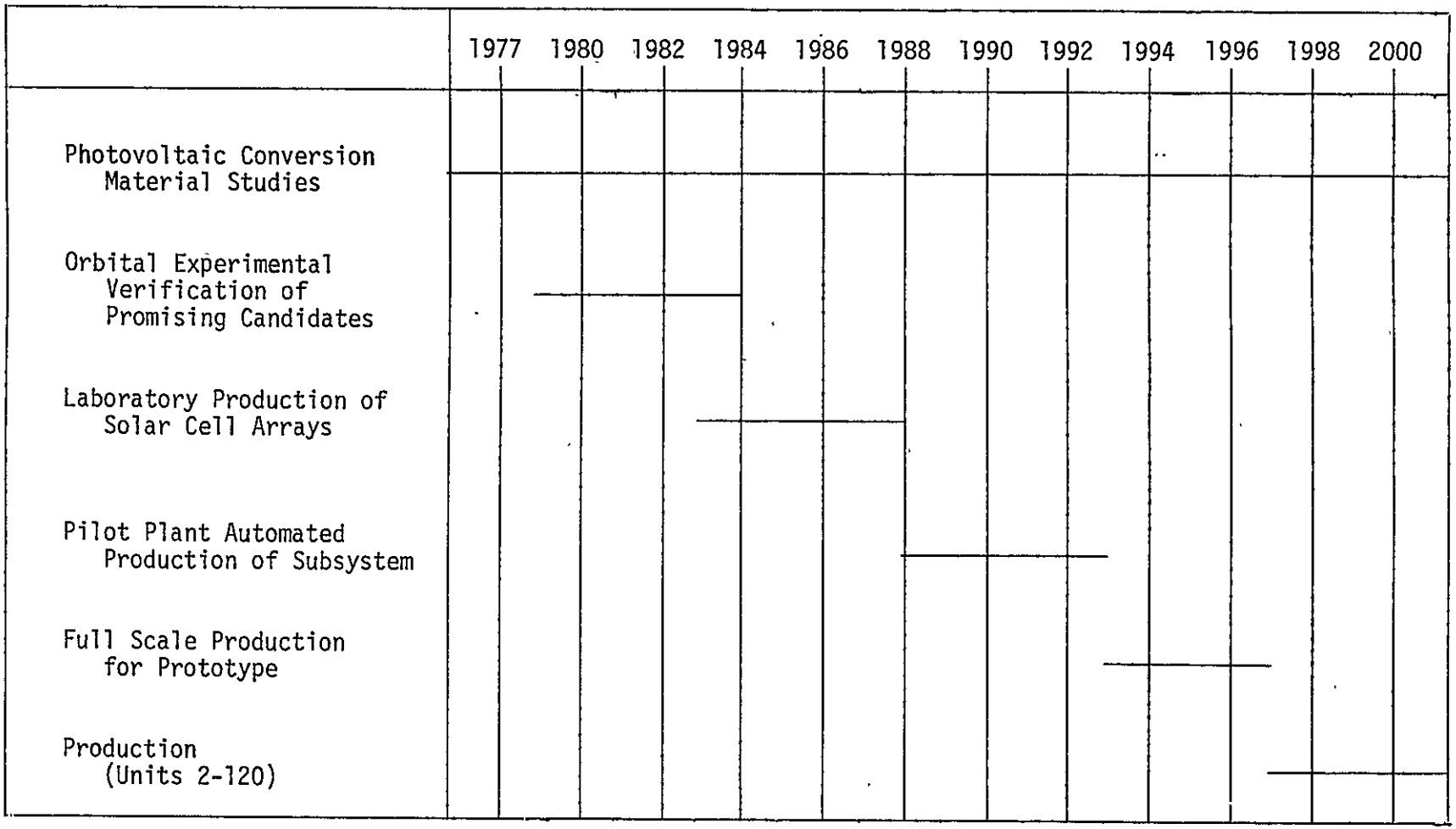

FIGURE 6.1 RECOMMENDED PROGRAM SCENARIO FOR THE INVESTIGATION AND DEVELOPMENT OF PHOTOVOLTAIC MATERIALS FOR THE SSPS

7. TECHNICAL DISCUSSION

This section discusses the significant aspects of the analytical (computer) model of the solar energy conversion subsystem, characteristics of the photovoltaic materials that were used in the model, and the analyses behind the choice of the particular optical reflector geometry used to provide concentrated sunlight.

7.1 Analytical Model

Figure 7.1 is a flow diagram of the computational sequence used in the analytical model of the solar energy conversion subsystem of the SSPS. The reason for developing the computer model was to describe the subsystem in sufficient detail to be able to compute the area of solar cells and optical reflectors needed to provide 5 GW of generated power to the utility interface as a function of the characteristics of each particular cell. Because the subsystem is but one part of the full SSPS system, it was necessary to make assumptions regarding the characteristics of the other subsystems for the SSPS. These assumptions were based upon the analyzed configuration of the SSPS, developed during an earlier phase of this current work, and were held constant throughout these analyses.

The analytical model is initially given an input parameter that defines for the program which set of solar cell descriptive data, stored internal to the program, is to be used for the current computation. In addition, the input data sets a minimum and maximum concentration ratio as well as the step size to be used in analyzing the intervening range of concentration ratios. For the particular concentration ratio being analyzed, the program will compute the geometry of the optical reflectors and the optical efficiency of the assumed optical reflecting surfaces. Next, the temperature of an individual solar cell is computed. This computation requires an iterative solution for the computation of cell efficiency, because the efficiency is temperature dependent. Additional factors in the computation of cell efficiency are the radiation damage at GEO, the incident angle of illumination, and the intensity of illumination.

Given the solar cell efficiency and the packing factor for assembling solar cells into an array, the total area of the solar cell array and reflecting surfaces are computed. The packing factor for assembling individual reflector/array modules into the solar energy conversion subsystem is then computed for the specific concentration ratio, as part of the computation of total area of the support structure.

The mass of the solar cell array is determined from the total area of the solar cell array multiplied by the mass per unit area of the particular cell being analyzed. The mass of the optics and basic support structure (which includes both conducting and non-conducting materials)

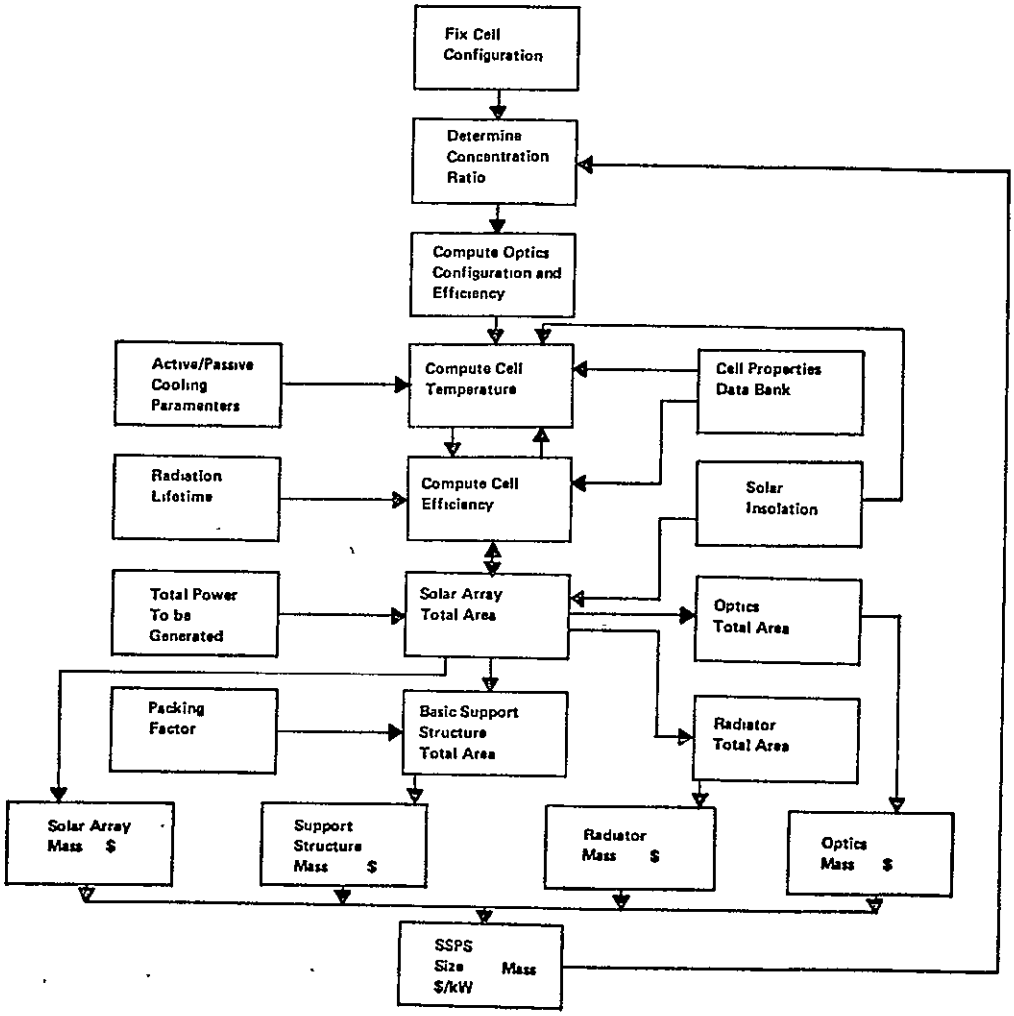

FIGURE 7.1 FLOW DIAGRAM OF COMPUTATIONAL SEQUENCE FOR ANALYTICAL MODEL OF SOLAR ENERGY CONVERSION SYSTEM

is determined from the computed areas of these elements multiplied by a fixed multiplier that represents the mass per unit area of each element.

When augmented cooling is considered in the analyses, an additional area parameter is included that is multiplied by the solar cell array area to compute the total radiator area and, at a later point, the total mass of the radiating surfaces. An additional "fin effectiveness" parameter is also introduced which defines the relative quantity of heat that is being rejected by the radiator, as designed, to the heat that could be rejected if the full radiator were at a uniform temperature equal to that of the solar cell array. The masses of the individual components are summed and the total mass multiplied by the transportation cost to GEO to obtain a total transportation cost. The capital cost of the individual components are summed and added to the transportation cost to obtain a single cost value for the 5 GW of power at the utility interface. This cost is not discounted in these analyses.

7.2 Photovoltaic Material Properties

The characteristics of the silicon, gallium arsenide and cadmium sulfide solar cells were obtained from a survey of the literature as well as from discussions with selected photovoltaic specialists. The basic properties that were cataloged are cell efficiency, mass per unit area and cost per unit area and these properties are tabulated in Section 4.0. To be able to compute cell efficiency as a function of concentration ratio required, in addition, a functional relationship for the dependence of conversion efficiency on temperature, illumination intensity and radiation damage. The following subsection defines the data representative of each cell and its source as used in the model.

7.2.1 Silicon Solar Cell

The current silicon solar cell is a single crystal, diffused junction cell that can be grown by one of several processes and is cut to the desired thickness. A 150 μm coverslide is typically used for protection against radiation damage. When this cell thickness is on the order of 200-300 μm, this configuration makes a very massive solar array, one that is not competitive with alternative cell configurations being considered for the SSPS. Thinner, single crystal silicon solar cells are being fabricated, with Lindmayer [6] having recently reported on the fabrication of a 50 μm silicon cell using a hot NaOH etching process on a thicker silicon sample. In addition, polycrystalline cells and thin film Schottky Barrier amorphous silicon cells [7] are being developed. Our current analyses are based upon single crystal, silicon solar cells with thickness ranging from 50 μm to 300 μm. Assumed coverslide thicknesses ranged from 25 μm to 150 μm; however, the rate of performance degradation due to radiation damage was not varied in the analytical model as a function of coverslide thickness. Only the mass of the cell changed as different coverslides were modeled.

The degradation in cell efficiency caused by increasing temperature, variations in illumination intensity, and radiation damage were typically reported in the literature by independent investigators using cells having different efficiencies at AMO and 26°C. To use this data in a unified analysis of the solar energy conversion subsystem required that each contributing factor to a change in cell efficiency be normalized and then multiplied, in series, by the basic efficiency (AMO at 26°C) of the cell being modeled.

7.2.1.1 Conversion Efficiency as a Function of Temperature

The data representing the change in efficiency of a silicon solar cell as a function of temperature was taken from the results of the flight qualification program of the violet solar cell as reported by Gaddy [8]. Figure 7.2 shows the variation in cell efficiency as a function of temperature for the three different solar cell materials.

7.2.1.2 Conversion Efficiency as a Function of Illumination Intensity

The relationship between conversion efficiency of a silicon cell and the intensity of solar illumination at normal incidence was taken from the work of Schueler et. al. [9]. Figure 7.3 shows this dependence for the three different cell materials.

7.2.1.3 Conversion Efficiency as a Function of Radiation Damage

The rate of degradation of cell performance as a function of equivalent fluence of 1 MeV electrons was taken from the review paper by Curtin and Statler [1] and is based on a covered INTELSAT IV cell manfactured from nominal 10 Ω • cm silicon. The data is shown in Figure 7.4

7.2.2 Gallium Arsenide Solar Cell

The basic gallium arsenide solar cell considered in this task is a gallium aluminum arsenide/gallium arsenide heterojunction with a single crystal gallium arsenide for the n region. Because gallium arsenide is a direct band gap material, the cell thickness can be less that that of a silicon cell. In our analyses, we have modeled gallium arsenide crystal thicknesses in the range of 5-10 μm [11]. A standard 125 μm FEP coverslide was assumed for the "most likely" mass per unit area configuration.

7.2.2.1 Conversion Efficiency as a Function of Temperature

The data representing the change in efficiency of a gallium arsenide solar cell as a function of temperature was taken from the work of Heinbockel and Roberts [11] and is shown in Figure 7.2

7.2.2.2 Conversion Efficiency as a Function of Illumination Intensity

The data representing the change in efficiency of a gallium arsenide solar cell as a function of illumination intensity was taken from the report by Heinbockel and Roberts [11].

7.2.2.3 Conversion Efficiency as a Function of Radiation Damage

The critical fluences for electron and proton irradiation of gallium arsenide and silicon solar cells were documented in Hovel's book on solar cells [12] with credit given to Wysocki [3] as the original source. Based upon the tabulated data for an electron particle energy of 0.8 MeV, the ratio of the critical fluence of GaAs cell to a silicon cell was 0.85. In the analytical model, this multiplier was used with the functional form of a silicon cell degradation which had been derived for an equivalent fluence of 1 MeV electrons.

7.2.3 Cadmium Sulfide Cell

Stanley's [4] work is a good review document on cadmium sulfide solar cells as is Hovel's [12] book. In our modeling of a copper sulfide/cadmium sulfide heterojunction cell, we have considered a 2-5 μm thick layer of CdS as the material. The mass of the cell is dominated by the assumed 25 μm thick SiO_2 coverglass (43% of total mass) and the 50 μm thick Kapton substrate (48% of total mass). Of the three materials considered, the thin film, polycrystalline, cadmium sulfide cell has the greatest potential for mass production, based on projection of the present state-of-the-art, as it does not require the controlled growth of a single crystal as do our assumed (for this task) silicon and gallium arsenide cells.

7.2.3.1 Conversion Efficiency as a Function of Temperature

The rate of change of conversion efficiency of a cadmium sulfide cell as a function of temperature was modeled as -0.036 %/°C as documented by Nakayama [15].

7.2.3.2 Conversion Efficiency as a Function of Illumination Intensity

No data was found for the variation in conversion efficiency as a function of illumination intensity so this effect was not included in the analytical model for cadmium sulfide.

7.2.3.3 Conversion Efficiency as a Function of Radiation Damage

Statler [18] has reported that no degradation in cell conversion efficiency was measured after a CdS cell was irradiated with a

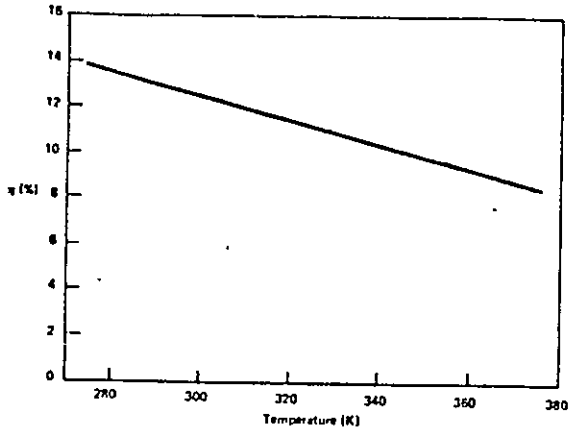

SILICON

GALLIUM ARSENIDE

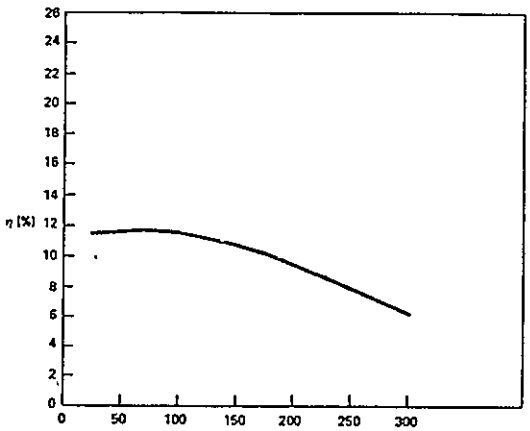

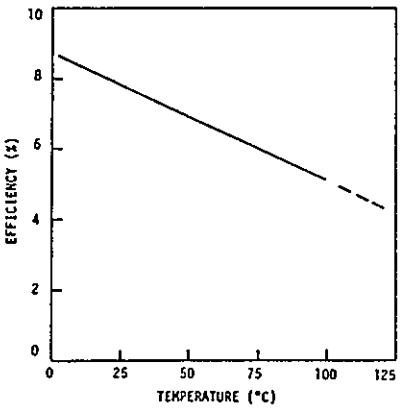

CADMIUM SULFIDE

FIGURE 7.2 VARIATION IN CELL CONVERSION EFFICIENCY (η) AS A FUNCTION OF TEMPERATURE (°C) FOR THREE DIFFERENT SOLAR CELL MATERIALS

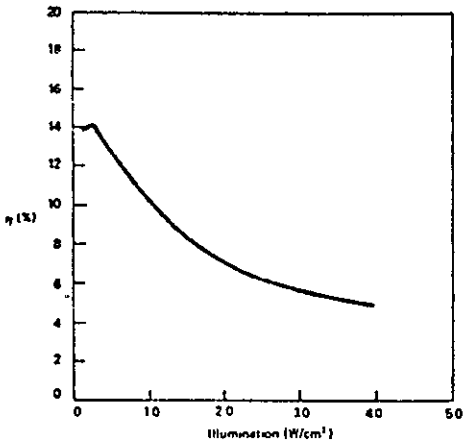

SILICON

GALLIUM ARSENIDE

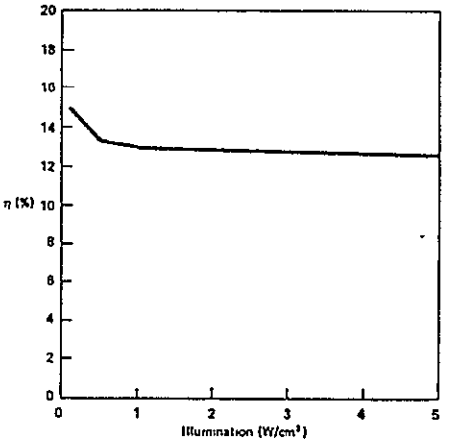

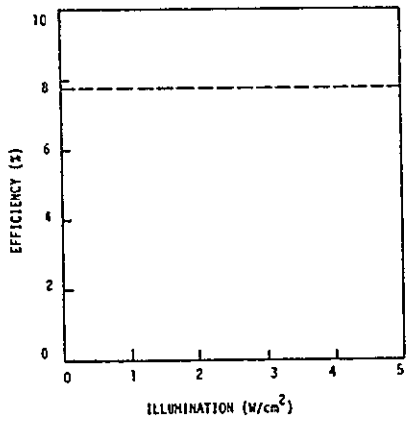

CADMIUM SULFIDE

FIGURE 7.3 VARIATION IN CELL CONVERSION EFFICIENCY (η) AS A FUNCTION OF INTENSITY OF ILLUMINATION FOR THREE DIFFERENT SOLAR CELL MATERIALS

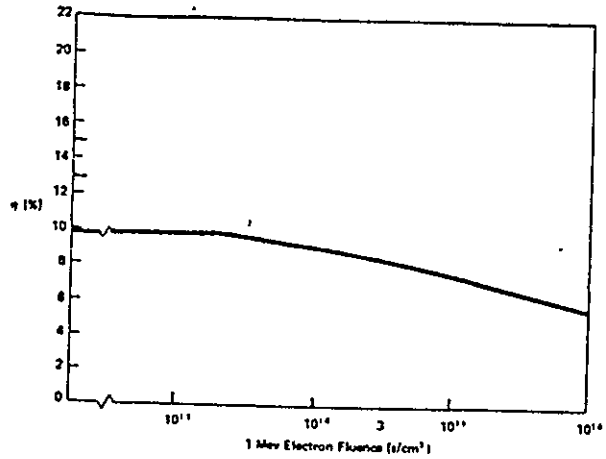

SILICON

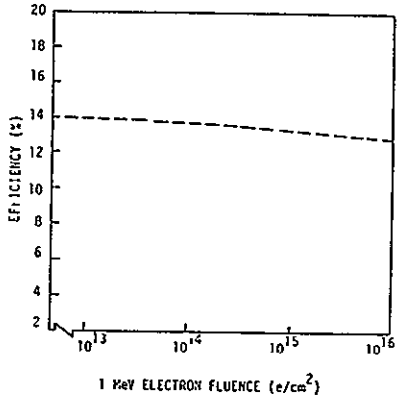

GALLIUM ARSENIDE

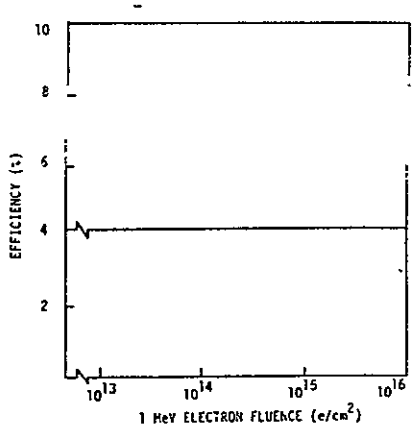

CADMIUM SULFIDE

FIGURE 7.4 VARIATION IN CELL CONVERSION EFFICIENCY (η) AS A FUNCTION OF RADIATION DAMAGE FROM 1 MeV ELECTRON FLUENCE FOR THREE DIFFERENT SOLAR CELL MATERIALS

fluence of 10^{16} e/cm^2 of 1 MeV electrons. Brandhorst [17] has also reported no cell degradation over a range of electron and proton energy levels. Both investigators commented on the darkening of the mylar or Kapton coverslide used in the tests. In our analytical model, we have assumed no degradation in cell performance due to particle radiation at GEO for a cadmium sulfide cell.

7.3 Optical System Analyses

7.3.1 Geometric Configuration of Optics

To be able to vary the concentration of sunlight falling on the solar cells and to compute the resulting area and mass of the optical systems required a definition of the reflector geometry for each theoretical concentration ratio.* Figure 3.2 showed fifteen proposed SSPS configurations and Figure 7.5 summarizes seven basic geometric configurations taken from the optical reflectors in the proposed systems. The philosophy established for the optical reflectors in the analytical model was to minimize the area of reflecting surface at each concentration ratio. It is obvious that each planar facet of the reflector system can, theoretically, increase the intensity of sunlight falling on the solar array by no more than one sun. Therefore, the number of planar facets in the optical system is a measure of the maximum theoretical concentration ratio attainable with that configuration. It is also true that, for a front-lit system, the reflecting system grows very long in the direction of the sun as one approaches their theoretical limit of concentration. For this reason, a smaller ratio of reflecting surface area to solar array is attained by increasing the number of planar mirrors in the system. A disadvantage of more mirrors in a front lit system is that the cell is illuminated at angles further off normal and this results in a decrease in cell absorptance. In this task, we have assumed minimum area for the optical system and computed the resulting optical inefficiencies. Table 7.1 summarizes the analytical expressions derived for the ratio of mirror area to solar cell area for the seven candidate geometries shown in Figure 7.5. Figure 7.6 is a plot of these analytical expressions. Based upon the goal to minimize the ratio of mirror area to solar cell array area, the geometric configurations shown in Figure 7.7 were incorporated in the analytical model.

7.3.2 Efficiency of Optical System

The optical system, as modeled, had two additional effects that increase size and mass of the SSPS other than its own mass penalty. First the assumed vapor deposited aluminum (VDA) reflecting surface is not a perfect reflector and has a solar absorptance that is dependent on angle of illumination. Figure 7.8 shows the variation in angle and size of single reflector surface as a function of concentration ratio and

---

*Theoretical concentration ratio as used herein is the ratio of the total projected area of reflectors plus solar cell array to the projected area of the solar cell array.

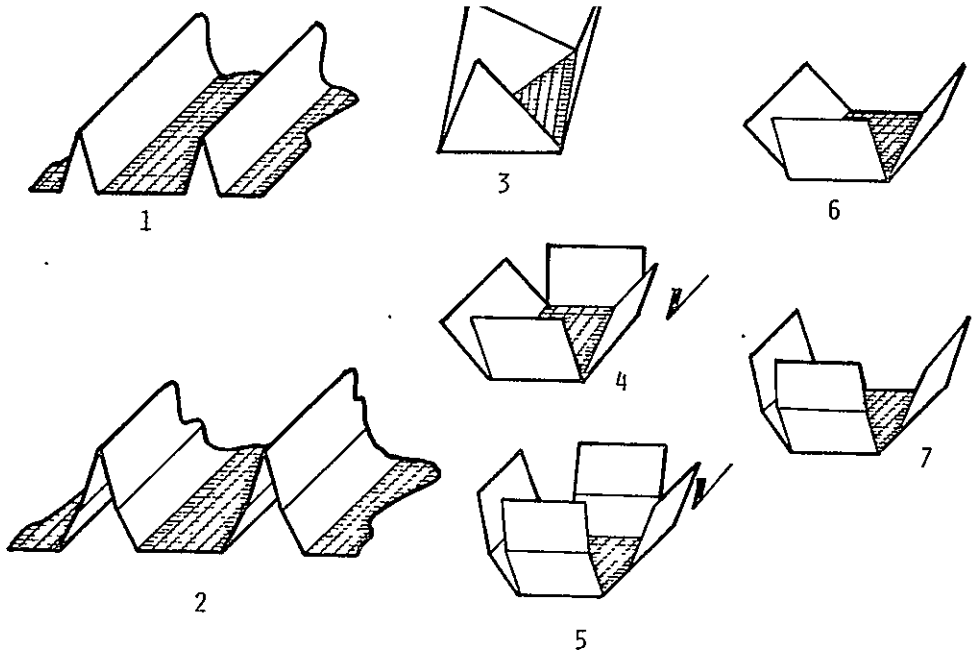

FIGURE 7.5 TYPICAL OPTICAL CONFIGURATIONS

Table 7.1 Ratio of Mirror Area to Solar Cell Array Area for Candidate Systems

Candidate	Ratio of Mirror Area to Array Area
1. 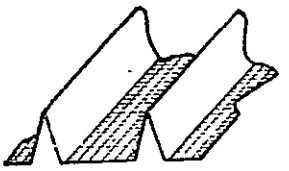	$\frac{2 \cdot (CR - 1)}{\sqrt{3 - CR}}$
2. 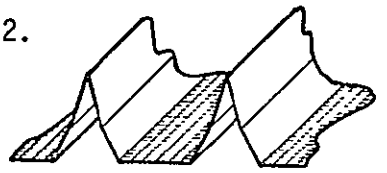	$\frac{2}{\cos(\alpha)} (\sin^2\alpha - \cos^2\alpha) + \frac{2 \cdot \sqrt{2} \sin(\alpha)}{\sqrt{1 - \sin(\alpha)}}$ where $\sin(\alpha) = \frac{-1 + \sqrt{5 + 4 \cdot CR}}{4}$
3. 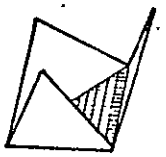	$(CR - 1) \cdot \sqrt{\frac{6}{(4 - CR)}}$
4. 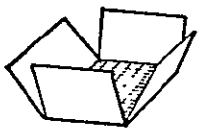	$(CR - 1) \cdot \sqrt{\frac{8}{(5 - CR)}}$

Table 7.1 Ratio of Mirror Area to Solar Cell Array Area for Candidate Systems (continued)

Candidate	Ratio of Mirror Area to Array Area
5. 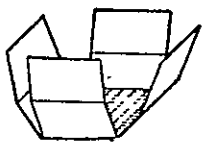	$4 \cdot \left(\frac{2 \cdot \sin^2(\alpha) - 1}{\cos(\alpha)} + \frac{\sqrt{2} \cdot \sin(\alpha)}{\sqrt{1-\sin(\alpha)}} \right)$ where $\sin(\alpha) = \frac{\sqrt{7 + 2 \cdot CR} - 1}{4}$
6. 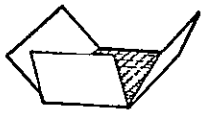	$(CR - 1) \cdot \sqrt{\frac{6}{4 - CR}}$
7. 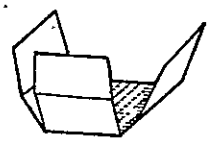	$3 \cdot \left(\frac{2 \cdot \sin^2(\alpha) - 1}{\cos(\alpha)} + \frac{\sqrt{2} \cdot \sin(\alpha)}{\sqrt{1 - \sin(\alpha)}} \right)$ where $\sin(\alpha) = \frac{-3 + \sqrt{57 + 24 \cdot CR}}{12}$

CR ≡ Theoretical Concentration Ratio

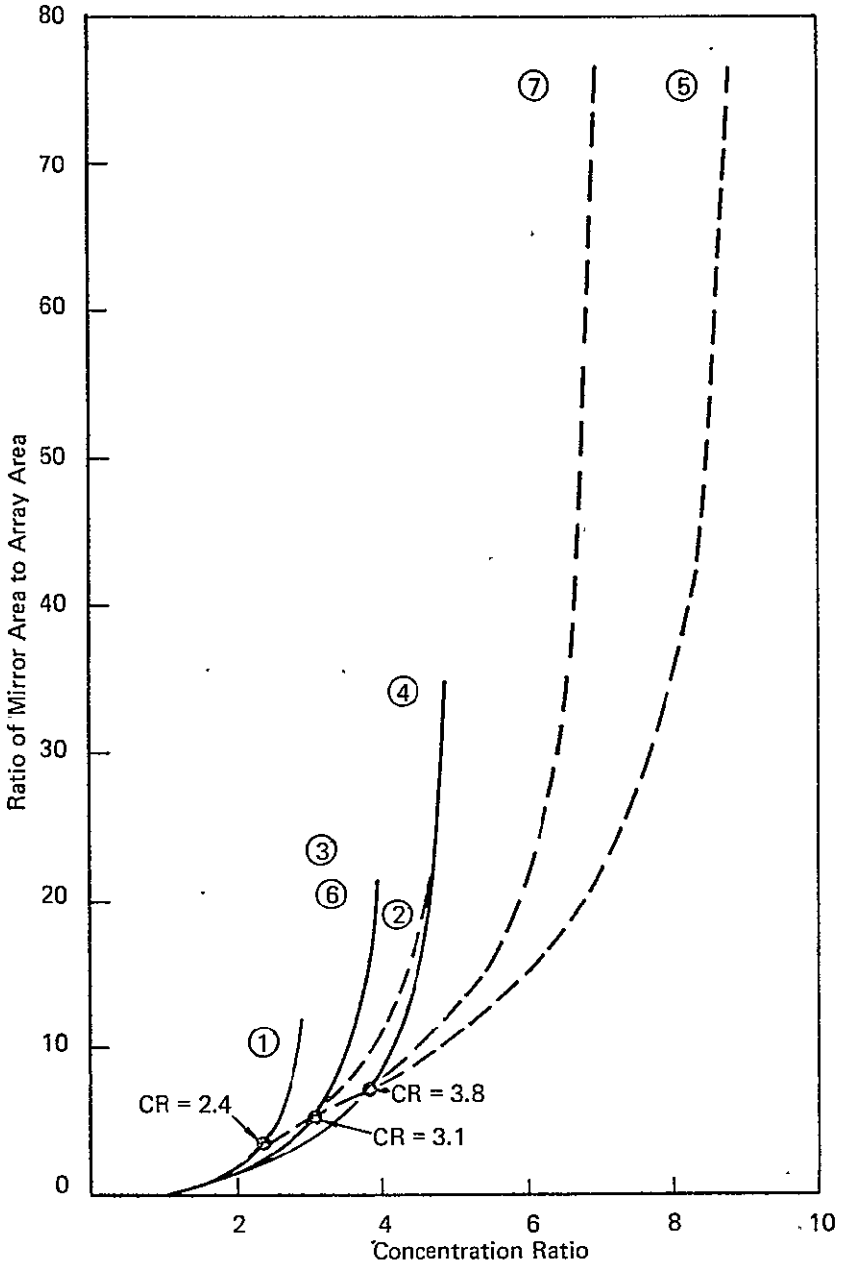

FIGURE 7.6 RATIO OF MIRROR AREA TO CELL AREA AS A FUNCTION OF CONCENTRATION RATIO FOR A FRONT LIT SSPS WITH DIFFERENT MIRROR CONFIGURATIONS
OPTICAL SYSTEM EFFICIENCY=1.0

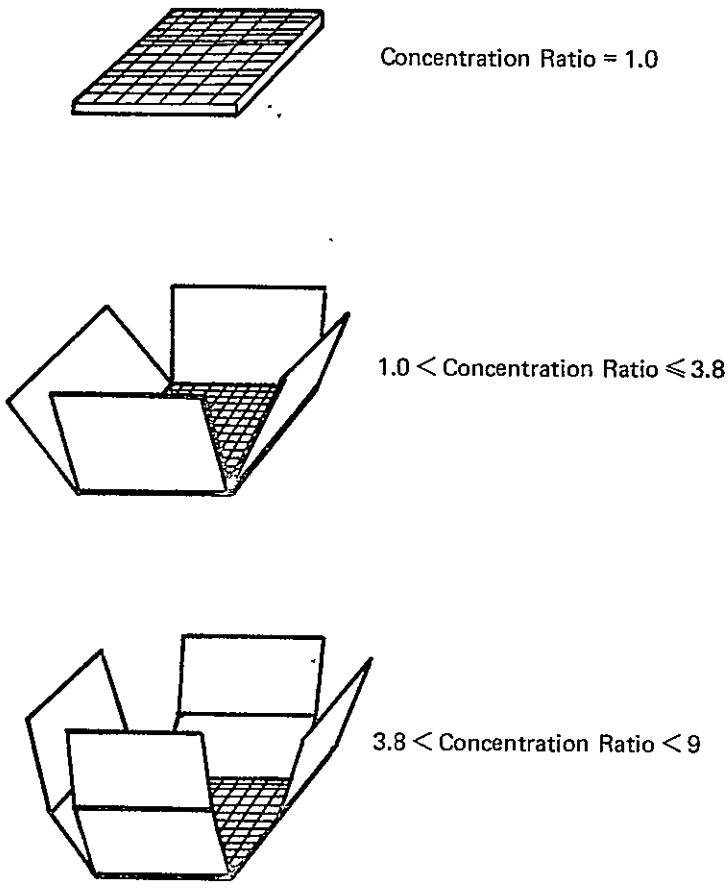

FIGURE 7.7 GEOMETRIC CONFIGURATION OF OPTICAL REFLECTORS FOR INCREASING CONCENTRATION RATIO OF SOLAR ENERGY

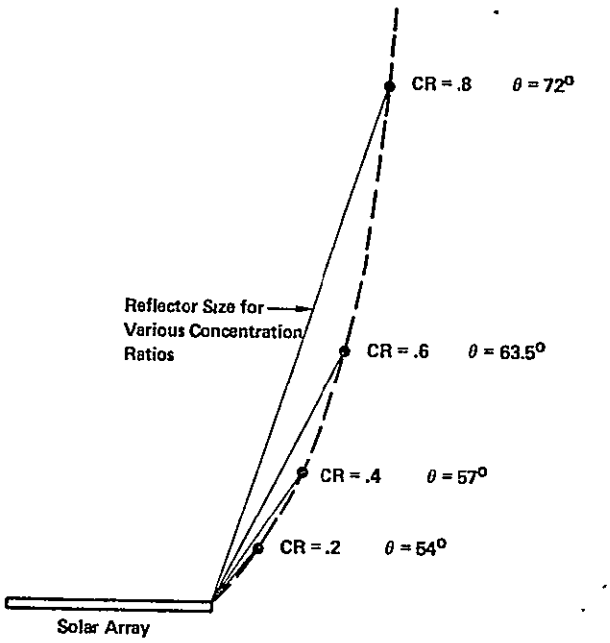

FIGURE 7.8 ANGLE AND SIZE OF A SINGLE REFLECTOR FOR VARIOUS CONCENTRATION RATIOS

Figure 7.9 shows the solar absorptance of VDA as a function of angle of incidence [18]. This angle dependence of solar absorptance shown by VDA is incorporated in the analytical model. The second effect is that individual modules of reflectors and solar cell array do not pack tightly together. There is an unused projected area of the basic support structure at each common point of a cluster of four adjacent reflectors/array modules that is modeled as a mass penalty due to the presence of the (assumed) continuous basic support structure with no local conversion of solar energy. This mass penalty is modeled as a packing factor (PF) for the reflector/array module situated in the basic support structure and is given by:

$$PF = \frac{4 \cdot CR}{(CR+1)^2}$$

where CR = theoretical concentration ratio.

7.3.3 Optical Efficiency of Solar Cell

There is a variation in the solar absorptance of a solar cell/coverslide as a function of the angle of incidence of the solar energy. Figure 7.10 shows this variation for both a fused silicon cell (coverslide) with no coating [19] and for the COMSAT Non-Reflecting (CNR) cell [20]. The use of a textured surface or an anti-reflection coating to increase the solar absorptance of the cell at a normal angle of incidence will result in a more significant relative decrease in conversion efficiency for off normal angles of illumination than is obtained with an untreated cell [19]. The analytical model assumes for all cells a variation in solar absorptance as a function of angle based upon the data for the CNR cell.

7.4 Thermal Analyses

In all of the analyses made with the deterministic model of the energy conversion subsystem, the solar energy absorbed by a given area of the array, and not converted to electrical energy, was assumed to be radiated off the front and back surfaces of the same array. The solar absorptance of the solar cell array was assumed to be 0.85 and its IR emittance, 0.80. The IR emittance of the backside of the array substrate was assumed to be 0.90. An analysis, independent of the subsystem model, considered an alternative passive cooling scheme. Figure 7.11 shows a view of a conducting substrate for the solar array that also serves as the optical reflector for concentrating the sunlight. In order to reduce the temperature gradients in the substrate, while keeping the mass of the substrate small, the lateral dimension of an individual solar cell string was assumed to be 2 centimeters.

The advantage of this design approach is that the backside of the reflectors can be given a high IR emittance and serve as additional radiating area, thereby reducing the temperature of the solar cell array and increasing its efficiency.

Two disadvantages of this approach are (1) the additional mass of the conducting substrate and (2) the non-continuous layout and interconnection of the solar cell array (in two dimensions) which would produce added difficulties in the mass production of the array.

The graph in Figure 7.11 shows the computed efficiency of a silicon cell as a function of the thickness of its aluminum substrate. An increase in thickness of the substrate results in a decrease in cell temperature up to a thickness at which the substrate is essentially isothermal. This occurs, for the assumed 2 centimeter width of the solar cell string, at a substrate thickness of about 25 μm (.001 inch).

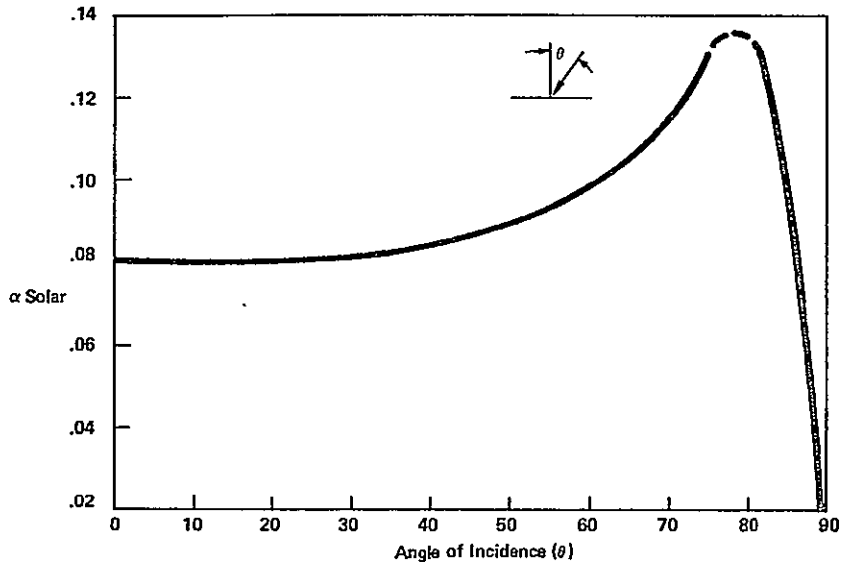

FIGURE 7.9 SOLAR ABSORPTANCE OF VAPOR DEPOSITED ALUMINUM (VDA) AS A FUNCTION OF ANGLE OF INCIDENCE

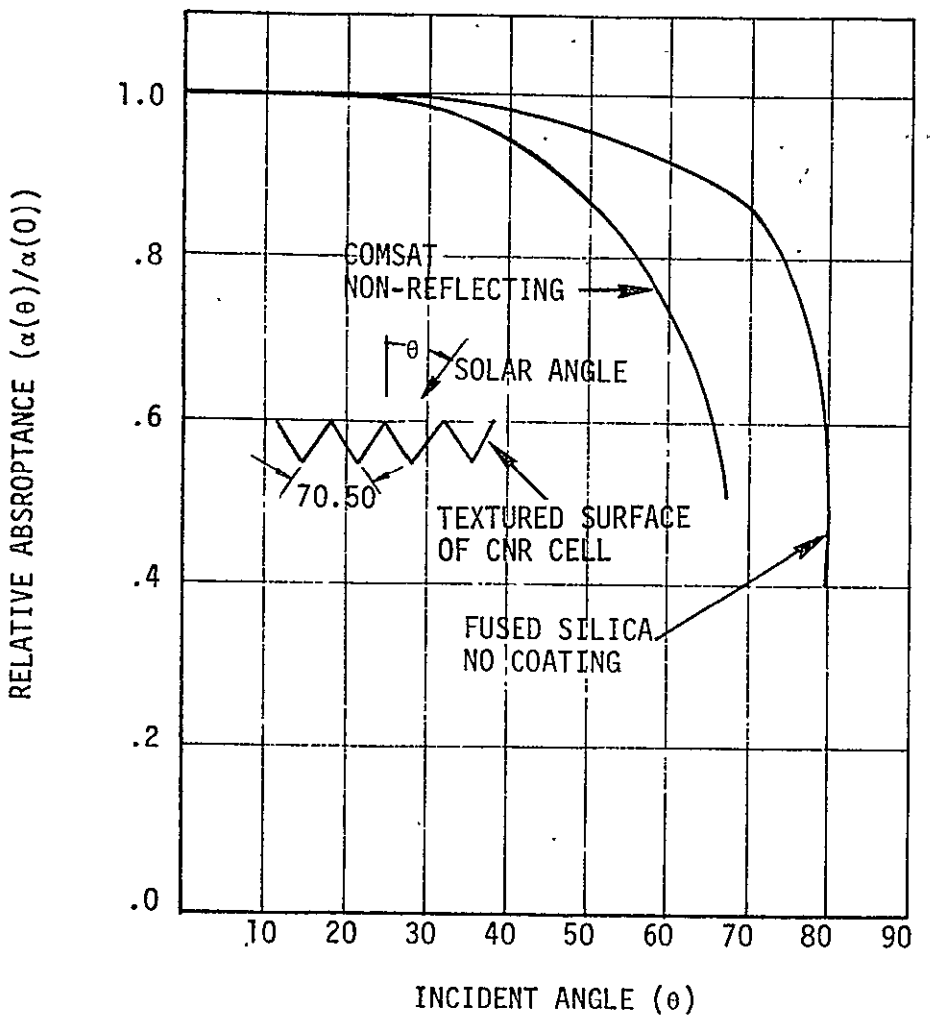

FIGURE 7.10 VARIATION IN SOLAR ABSORPTANCE OF CELL AS A FUNCTION OF ANGLE OF INCIDENCE

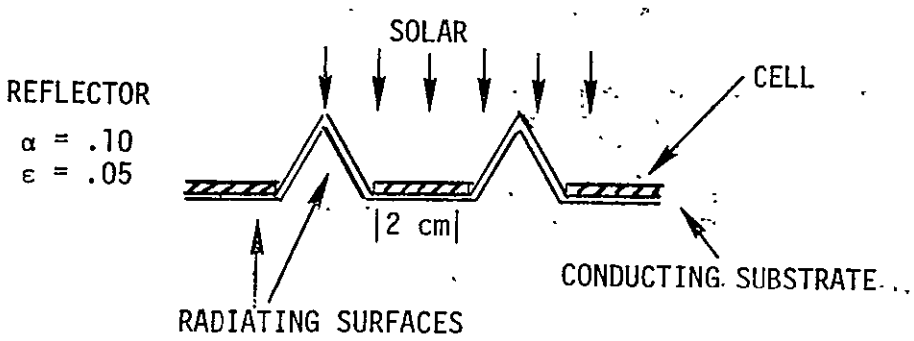

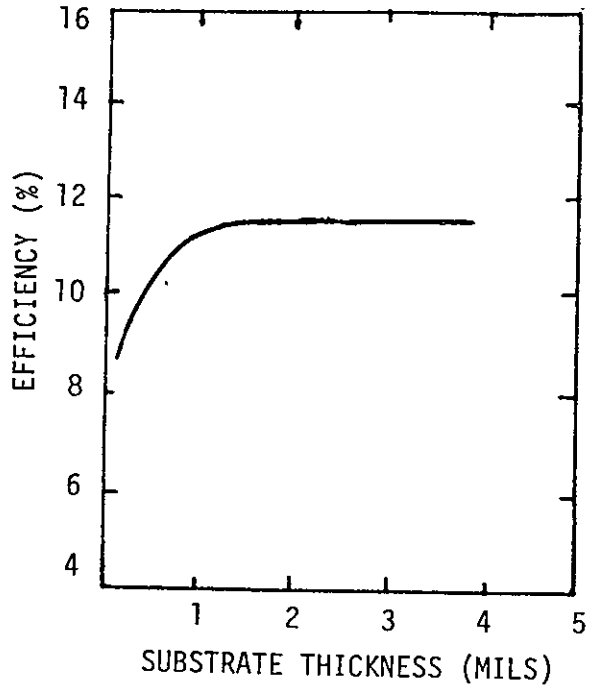

FIGURE 7.11 COMPUTED EFFICIENCY OF A SILICON CELL AS A FUNCTION OF THE THICKNESS OF ITS ALUMINUM SUBSTRATE

REFERENCES

1. Curtin, D. J. and Statler, R. L., Review of Radiation Damage to Silicon Solar Cells, IEEE Transaction on Aerospace and Electronics Systems, Volume AES-11, No. 4, July 1975.

2. Waddel, R., Solar Cell Radiation Damage on Synchronous Satellites ATS-1 Proceedings Seventh IEEE Photovoltaic Specialits Conference, pp. 195-205, 1968.

3. Anspauch, B. E., ATS-4 Solar Cell Experiment after 699 Days in Synchronous Orbit, Proceedings Ninth IEEE Photovoltaic Specialists Conference 1972.

4. Private Communication with M. Field at Pantek International Corporation Lewistown, Pennyslvania.

5. Rauschenbach, H. S. and Cannady, M. D., Final Report Flexible, FEP Teflon Covered Solar Cell Module Development, prepared for NASA Lewis Research Center, Contract NAS 3-16742, October 1976.

6. Lindmayer, J. and Wrigley, C., A New Lightweight Solar Cell, Twelth IEEE Photovoltaic Specialists Conference, 1976.

7. Wronski, C. R., Carlson, D. E., and Daniel, R. E., Schottky Barrier Characteristics of Metal-Amorphous Silicon Diodes, Applied Physics Letters, Volume 29, No. 9, 1 November 1976.

8. Gaddy, E. M., Flight Qualification Test Results for Violet Cells, Proceedings Tenth IEEE Photovoltaic Specialists Conference, pp. 153-162, 1973.

9. Schueler, D. G., et.al., Integration of Photovoltaic and Solar-Thermal Energy Conversion Systems, Proceedings Eleventh IEEE Photovoltaic Specialists Conference, p. 331, 1975.

10. Walker, G. H., Third Working Meeting on Gallium Arsenide Solar Cells, NASA Langley Research Center, N 76-21681, September 1975.

11. Heinbockel, J. H. and Roberts, A. S., Jr., Analysis of GaAs and Si Solar Energy Hybrid Systems, Final Report for NASA Langley Research Center, December 1975.

12. Hovel, Harold J., Semiconductors and Semimetals, Volume 11, Solar Cells, Academic Press, 1975.

13. Wysocki, J. J., Journal Applied Physics, 34, 2915 (1963).

14. Stanley, A. G., Cadmium Sulfide Solar Cells, Applied Solid State Science, Volume 5, Academic Press, 1975.

15. Nakayama, N., Ceramic CdS Solar Cell, Japanese Journal of Applied Physics, Volume 8, No. 4, p. 450, 1969.

16. Schaefer, J. C., Proceedings Third Photovoltaic Specialists Conference Report, No. PIC-SOL-209/3 (1963).

17. Brandhorst, H. W., Jr., Radiation Effects, Cadmium Sulfide Thin Film Solar Cell Cell Review, NASA TMX-52579, p. 102 (1968).

18. Hoke, M. G., A Thermal Vacuum Technique for Measuring the Solar Absorptance of Satellite Coatings as a Function of Angle of Incidence, AIAA Journal, Volume 3, No. 5, pp. 947-951, (1965).

19. Jet Propulsion Laboratory, Solar Cell Array Design Handbook, Volume I, p. 48-1, October 1976.

20. Arndt, R. A., et.al., Optical Properties of the COMSAT Non-Reflecting Cell, Proceedings Eleventh IEEE Photovoltaic Specialists Conference, p. 43, 1975.

☆U.S. GOVERNMENT PRINTING OFFICE 1977—740—049/295 REGION NO. 4